PNAS
www.pnas.org

Supplementary Information
for

Scalable, Economical, and Stable Sequestration of Agricultural Fixed Carbon

(Agricultural Carbon Capture and Sequestration: Agro CCS)

Authors & Author Affiliation:

Eli Yablonovitch & Harry Deckman,

Department of Electrical Engineering and Computer Science, University of California, Berkeley, CA 94720;

Corresponding Author: Eli Yablonovitch eliy@eecs.berkeley.edu

This PDF file includes:

Supplementary Text

1. Preservation of Biological Carbon Using Agro-Sequestration and Comparison With Other Technologies that Photosynthetically Capture Carbon
    - 1.1 Empirical evidence for long term biomass sequestration in dry environments.
    - 1.2 How water activity in the stored biomass of less than 0.6 can be achieved.
    - 1.3 How salts can be helpful in maintaining a dry environment within the engineered dry biolandfill.
    - 1.4 Problems with biomass preservation in other environments.
    - 1.5 Comparison of dry biomass storage (Agro-Sequestration) with other technologies that photosynthetically capture carbon.
2. Dry Biolandfill Technology
3. Candidate crops and biomass availability
    - 3.1 Candidate crops
    - 3.2 Biomass availability
4. Detailed Analysis of Costs for Growth and Sequestration of Miscanthus and Switchgrass
    - 4.1 Cost structure for establishment and growth of miscanthus
    - 4.2 Cost structure for establishment and growth of switchgrass
    - 4.3 Technology for anaerobic landfills and cost estimates
        - 4.3a *Technical basis for biolandfill design*
        - 4.3b *Technology to dry, compact, and sequester crops in the biolandfill*
        - 4.3c *Economic model of biolandfill CAPEX and OPEX for initial miscanthus and switchgrass projects*
    - 4.4 Summary of base case economics for growth and stable sequestration of miscanthus and switchgrass crops in biolandfills.
    - 4.5 Economic sensitivity analysis and implications for other miscanthus and switchgrass Agro-Sequestration technology options
5. Analysis of Agro-Sequestration Costs for Pine Trees
6. Scaling Relationships That Provide a Rough Estimate of Crop and Biolandfill Costs
7. Water Transport Through Cap and Base Water Permeation Barriers
8. Scenario for Sequestration of 500Megatonnes/Year of Biomass in the United States and Agro-Sequestration CO_2 Footprint
9. Experience Curves and a Moore's Law For Agriculture

Supplementary Figures

Figure S1.2a: Water adsorption branch isotherms at 25C for miscanthus, prairie cordgrass and an average of ten hardwoods.

Figure S1.2b: Miscanthus water adsorption branch isotherms at 20C, 25C, and 40C.

Figure S1.3a: Water adsorption branch isotherms at 25C for NaCl and $MgCl_2$.

Figure S1.3b: Water adsorption branch isotherm at 25C for $CaCl_2$

Figure S1.3c: Mass ratio of $CaCl_2$ salt to dry miscanthus versus mass ratio of total water contained in the biolandfill to dry miscanthus. Lines shown set the amount of salt needed to lower water activity to 0.6, 0.4 or 0.2

Figure S2.a Cross sectional view of biolandfill showing dry tomb structure.

Figure S2.b Detailed view of bottom seal in the dry tomb structure.

Figure S2.c Detailed view of top seal in the dry tomb structure.

Figure 4.5a Base case bottom-up analysis of Agro-Sequestration costs for miscanthus, switchgrass, and loblolly pine along with brackets covering a wide range of likely scenarios.

Figure S6.a The vertical axis shows inflation adjusted yearly farm revenue per hectare for corn, wheat, soybeans, and alfalfa hay derived from historical crop prices and yields, and the horizontal axis is the cumulative probability distribution. Median values are taken as representative of farm incomes that support different types of farming and are used to form a rough estimate of the agricultural CO_2 capture cost.

Figure S6.b Left axis gives median values taken from the cumulative probability distribution (shown in Figure S6.a) of inflation adjusted farm revenue per hectare. These median values are considered to be representative of revenue that supports different types of farming. A perspective on the market conditions under which farmers economically produce crops is shown with brackets that span the lower quartile to the upper quartile in the distributions of yearly farm income. The right axis scales the left axis to an equivalent agricultural CO_2 capture cost by assuming energy crop yield of 22.5 dry tonne/hectare and 50wt.% carbon content. The conversion factor from the right axis is 0.0243Hectares/CO_2-tonne-year. The right axis is a purely economic scaling and does not mean that

farmland used to grow food crops is used for Agro-Sequestration (see Section 6 of the SI).

Figure S9.1 There is a Moore's Law for agriculture, but it is much slower than the Moore's Law for transistor density. National governments have paid particular attention to agricultural land productivity. There is good data for wheat in Great Britain, going back hundreds of years. Wheat productivity in tonnes/hectare has been improving, through the "experience curve". Humanity has 10000years "experience" in agriculture. In the past 100years, the tonnes/hectare has doubled every 50 years, but we are conservatively basing our Agro-Sequestration cost estimates on current agricultural methods, and neglecting the inevitable future improvements.

Supplementary Tables

Table S.3 Examples of high productivity candidate Agro-Sequestration crops.

Table S4.1a Miscanthus pre-establishment costs for field preparation in excess of revenue from herbicide tolerant crop and winter oat cover crop in the year before rhizome planting.

Table S4.1b Miscanthus costs during year #1 in which rhizomes are planted.

Table S4.1c Miscanthus costs during year #2: first harvest (yield=1/2 of mature crop).

Table S4.1d Miscanthus costs for year #3+: harvests of mature crop.

Table S4.2a Switchgrass pre-establishment costs for field preparation in excess of revenue from herbicide tolerant crop and winter oat cover crop in the year before planting.

Table S4.2b Switchgrass costs during year #1 in which field is planted and first harvest conducted.

Table S4.2c Switchgrass costs during year #2: replanting and second harvest.

Table S4.2d Switchgrass costs for year #3+: harvests of mature crop.

Table S4.3a Biolandfill construction cost used as a base case estimate of Agro-Sequestration economics.

Table S4.3b Biolandfill closure cost used as a base case estimate of Agro-Sequestration economics.

Table S4.3c Estimated biolandfill operating costs (US$/tonne of crop sequestered) for early demonstration projects.

Table S4.4a Base case Agro-Sequestration cost summary for miscanthus. Cost of sequestered carbon is computed from the sequestered miscanthus price using 48wt.% carbon in dry miscanthus.

Table S4.4b Base case Agro-Sequestration cost summary for switchgrass. Cost of sequestered carbon is computed from the sequestered switchgrass price using 44wt.% carbon in dry switchgrass.

Table S5 Base case Agro-Sequestration cost summary for Loblolly pine. Cost of sequestered carbon is computed from the sequestered dry pine price using 50wt.% carbon in dry wood.

Table S8.1 Distribution of biomass sources for a hypothetical scenario sequestering 500 megatonnes/year of biomass with Agro-Sequestration in the US.

Table S8.2 Distribution of energy crops chosen from potential biomass additions by 2040 listed in DOE Billion Ton report [71].

Table S8.3 Distribution of agricultural residues chosen from potential biomass additions by 2040 listed in DOE Billion Ton report [71].

Table S8.4 Distribution of waste products chosen from potential biomass additions by 2040 listed in DOE Billion Ton report [71].

Table S8.5 Land requirements for production of miscanthus, switchgrass, and trees in scenario sequestering 500megatonnes of biomass.

Table S8.6 Physical characteristics of biolandfills dedicated to miscanthus, switchgrass, and trees.

Table S8.7 Heated drying requirements to obtain water activity <0.6 for two scenarios with different $CaCl_2$ additions. One scenario has a larger (2wt.%) $CaCl_2$ addition and the other has a smaller $CaCl_2$ addition (spot treatment and treatments near water transport barriers).

Table S8.8 Indirect emissions from drying biomass and adding 2wt.% $CaCl_2$ throughout the entire biolandfill. Indirect emissions are expressed as a percent of the ratio of the mass of CO_2 emitted to the mass of CO_2 captured by the sequestered biomass.

Table S8.9 Indirect emissions from drying biomass and adding a small amount of $CaCl_2$. in spot treatments and in regions near the water transport barriers.. Indirect

emissions are expressed as a percent of the ratio of the mass of CO_2 emitted to the mass of CO_2 captured by the sequestered biomass.

Table S8.10 Direct and indirect CO2 emissions from biolandfill construction and compaction of biomass.

References for SI

Supplementary Text

1. Preservation of Biological Carbon Using Agro-Sequestration and Comparison With Other Technologies that Photosynthetically Capture Carbon

Agro-Sequestration technology is designed to preserve almost 100% of cultivated plant or tree biomass in an anaerobic environment that will ultimately setup within a dry tomb biolandfill. When construction is completed, the environment within a dry tomb biolandfill will be aerobic and will transition over time to an anerobic environment. Dry tomb biolandfills are designed to maintain a water activity that is low enough to suppress growth of microorganisms that would decay stored biomass in either aerobic or anerobic environments. Suppressing growth of microorganisms by reducing water activity is a principle used world-wide for food storage in aerobic and anaerobic environments [1]. As water activity decreases from 1 to 0.75 (a value corresponding to water saturated with NaCl, fewer and fewer microorganisms can survive in aerobic as well as anerobic environments [2, 3, 4] and their metabolic rates slow. It is uncertain whether microorganisms that can live without sunlight at a water activity of 0.75 will degrade biomass and if degradation occurs whether the rates will be slow enough to be acceptable with mitigation procedures available for biolandfills. As such future studies are needed to establish if 0.75 is a sufficiently low enough water activity for stable long-term sequestration of biomass. Degradation can most certainly be arrested by establishing an even lower water activity in the biolandfill. In aerobic environments life ceases to be viable when water activity is lowered below 0.6 [5] and it is expected that a similar limit exists in anerobic environments. This is due to similar water sorption isotherms of cell wall materials and the fact that microorganisms must transport water across cell walls to take up nutrients as well as to excrete waste products. When the water activity outside the cell wall decreases it exerts an osmotic stress that inhibits sorption and the water transport needed to supply food as well as remove waste products from microorganisms. Without these life supporting functions microorganisms that would degrade biomass become dormant or die. As such our initial dry tomb biolandfill designs preserving nearly 100% of the

biomass target a water activity of less than 0.6 and we recognize that with further research designs with water activity near 0.75 may be viable.

The following subsections will cover:

1.1 Empirical evidence for long term biomass sequestration in dry environments.

1.2 How water activity in the stored biomass of less than 0.6 can be achieved.

1.3 How salts can be helpful in maintaining a dry environment within the engineered dry biolandfill.

1.4 Problems with biomass preservation in other environments.

1.5 Comparison of dry biomass storage (Agro-Sequestration) with other technologies that photosynthetically capture carbon.

1.1 Empirical Evidence for Long Term Biomass Sequestration in Dry Environments.

Empirical support for the idea that long term biomass degradation can be suppressed by dry storage comes in part from the viability of plant seeds stored in dry environments for decades to centuries [6, 7] and even millennia [8, 9]. Laboratory experiments and seed storage banks typically employ lower activities than we propose, however the water activity expected in natural experiments [8, 9] that have preserved genetic viability for millennia appear to be in the range we propose. The most convincing of these is a ~2000year old date palm seed that was successfully germinated [9] after recovery from excavations at Herod the Great's palace on Masada in Israel. It had been preserved without freezing in an environment where the ambient water activity in air is nearly in the range we propose. Another natural example is the preservation of DNA in 6,000 and 3,300year-old Citrullus seeds from Libya and Sudan [10].

Additional support comes from the preserved state of foods, honey and seeds recovered from Egyptian tombs [11, 12] as well as plant materials used in the construction of segments and beacon towers of the ancient Great Wall in dry areas of northwestern China [13].

1.2 Achieving Water Activity of Less Than 0.6 by Drying Biomass

Reducing biomass water content by drying is a key element of Agro-Sequestration. Biomass acts as a water sorbent and the amount of water in biomass is characterized by an isotherm. Under equilibrium conditions the isotherm relates water activity to the amount of water sorbed by the biomass. Isotherms for various biomasses based on literature data [14, 15, 16] are shown in Figure S1.2a. These isotherms show H_2O uptake at 25C as activity of water is increased in units of:

Weight fraction of H_2O sorbed = mass H_2O / (mass H_2O + mass dry biomass) Eq. S1.1

This type of isotherm in Figure S1.2a. is often referred to as an adsorption branch isotherm and is measured as water activity is increased from 0 to 1. Desorption branch isotherms for the different biomasses have some hysteresis due to the plant's pore structure and differ slightly from the adsorption branch isotherms shown in Figure S1.2a. Hysteresis inhibits water from leaving mesopores and some macropores in the biomass. This causes significant regions of desorption branch isotherms to lie above equivalent adsorption branch isotherms. As such at a given water activity the water content in the biomass will be higher in desorption compared with adsorption.

Figure S1.2a: Water adsorption branch isotherms at 25C for miscanthus, prairie cordgrass and an average of ten hardwoods.

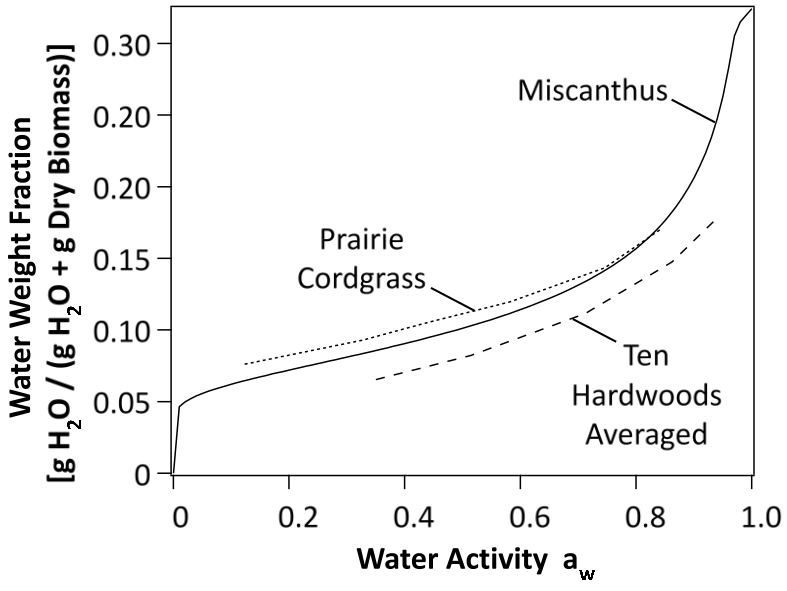

An adsorption branch isotherm for miscanthus (a highly productive energy crop) is shown over a full range of water activity in Figure S1.2a. At very low water activity (a_w<0.02) the water loading rises sharply due to water populating strongly bound sites.

In the region of interest for biomass storage (a_w ranging from 0.05 to 0.6), the amount of sorbed water rises gradually from about 5wt.% to 12wt.%. At high water activity ($a_w > 0.8$) loading of water rises much more rapidly due to filling of mesopores and macropores in miscanthus.

Figure S1.2a also shows water adsorption isotherms covering the region of interest for long term sequestration of prairie cordgrass and hardwood [16, 17]. The hardwood isotherm is an average for ten different hardwoods (Red Oak, White Oak, Yellow Poplar, Sweetbay, White Ash, Green Ash, Red Maple, and American Elm). It is seen that for water activities in the region of interest, the isotherms are qualitatively similar to miscanthus. This qualitative similarity extends to most other forms of biomass in part because the isotherm in this region is set by water adsorption into mesopores and micropores.

There is a modest temperature dependence for the thermodynamics of adsorption into mesopores and micropores and Figure S1.2b illustrates this with 20C, 25C, and 40C miscanthus water adsorption isotherms. It is seen that a significant portion of the difference between them comes from the temperature dependence of strongly adsorbed water that governs shape of the isotherm at low water activity (a_w<0.02). As such with a limited number of isotherms one can make quantitative estimates of the biomass dryness level required to store dried biomass at a given water activity. For example to store miscanthus at 25 C and a water activity of less

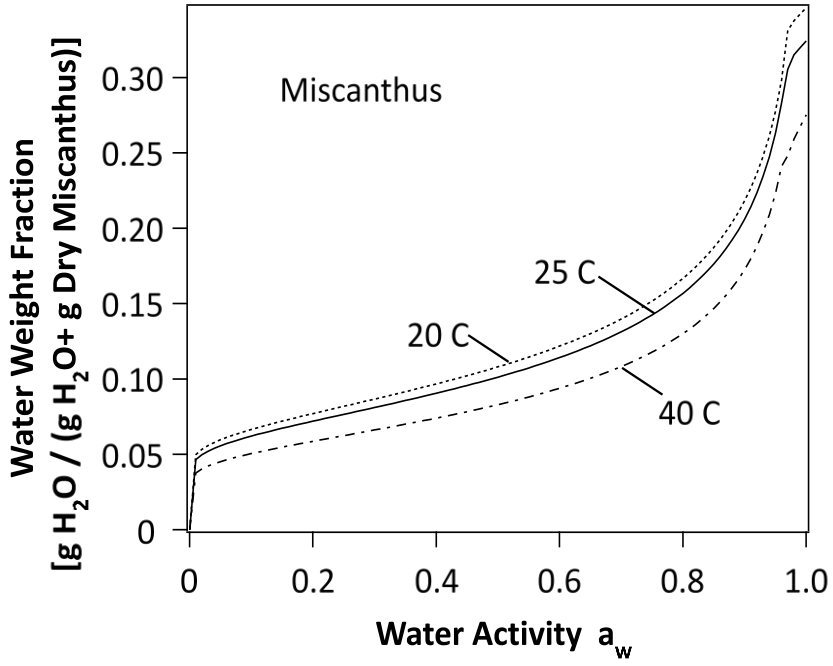

Figure S1.2b: Miscanthus water adsorption branch isotherms at 20C, 25C, and 40C.

than 0.6 it is seen that the miscanthus must be dried so that the water content is less than 11.5 g H2O/(g H2O+g dry miscanthus) or equivalently less than 12.9g H2O/g dry miscanthus. This water content can be achieved by heated drying and SI section 4 sets forth cost and energy requirements for drying along with a discussion of possible CO_2 emissions.

1.3 Assuring Low Water Activity With Salted Biomass

The hydroscopic and deliquescent nature of salt can make it a much higher capacity water sorbent than dried biomass. At low water activities the weight fraction of water sorbed by properly chosen salts can be more than 10 fold greater than dried biomass.

Salts can be used in a variety of ways within engineered biolandfills to help maintain a dry environment. Salt located near the walls of the dry tomb structure can mitigate the small diffusional influx of water through the water transport barriers forming the dry tomb. Spot treatments of salt during construction can help dry any water ingresses through seams in rain protective tarps. In the most conservative case, salt can be dispersed throughout the entire volume of biomass to help reduce the water activity. When salt is dispersed throughout the volume of the sequestered biomass it can be used for drying of the biomass, reducing the amount of thermal energy needed to remove water from the biomass, or to provide an extra degree of insurance preserving the dry tomb environment. In all these cases the biomass containing salt will be referred to as salted biomass. This salted biomass is a composite that can be a homogeneous or heterogeneous blend, mixture, interminglement, jumbling, or layering of biomass and salt.

Dry salt hydrates or deliquesces sorbing water and when there is sufficient water salt dissolves and forms solutions. In all states (solid or brine) salt draws and stores water molecules that otherwise would be free water or water sorbed into the biomass. Stable salts such as NaCl and $CaCl_2$ are not expected to react with biomass under sequestration conditions. The ability of salt to lower water activity is one of the reasons that NaCl has been commonly used as a food preservative. In addition, it is a disrupter that wreaks havoc in microbes that degrade food, interrupting their enzymes and chipping away at their DNA. This ability of alkali and alkaline earth metal salts to poison methane forming bacteria [18] led Amelse and Behrens [19] to suggest

using them to suppress biomass degradation in landfills although they did not consider them as desiccants. In our biolandfill designs the primary purpose for salting is to desiccate sequestered biomass. For biolandfills, salt levels and compositions that would not be acceptable for human consumption can be utilized to provide protection against water ingress during construction or long-term sequestration.

Water sorption isotherms as a function of increasing water activity can be used to quantify the reduction of water activity by salt in a dry tomb structure. Figure S1.3a replots literature data [20, 21, 22, 23] taken with increasing water activity in the form of water sorption isotherms for two common salts NaCl and $MgCl_2$. These salts are produced in large quantity and commonly used for road surface deicing.

Isotherms shown in Figure S1.3a are expressed in the same units as the biomass isotherms and similarly are adsorption branch isotherms that ignore any possible hysteresis. As the water activity increases from 0, no significant amount of water is sorbed until the water activity approaches the solubility limit. In the region where there is no significant amount of sorbed water (a_w=0 to <0.33 for $MgCl_2$ or a_w=0 to < 0.75 for NaCl) there can be hydrated or deliquesced salt. Close to the solubility limit, water content abruptly rises (or equivalently salt concentration decreases). In this region near the solubility limit where the water content abruptly rises there can be hydrated or deliquesced salt, saturated brine, or supersaturated brine. Values of water activity in this region near the solubility limit where

Figure S1.3a: Water adsorption branch isotherms at 25C for NaCl and $MgCl_2$.

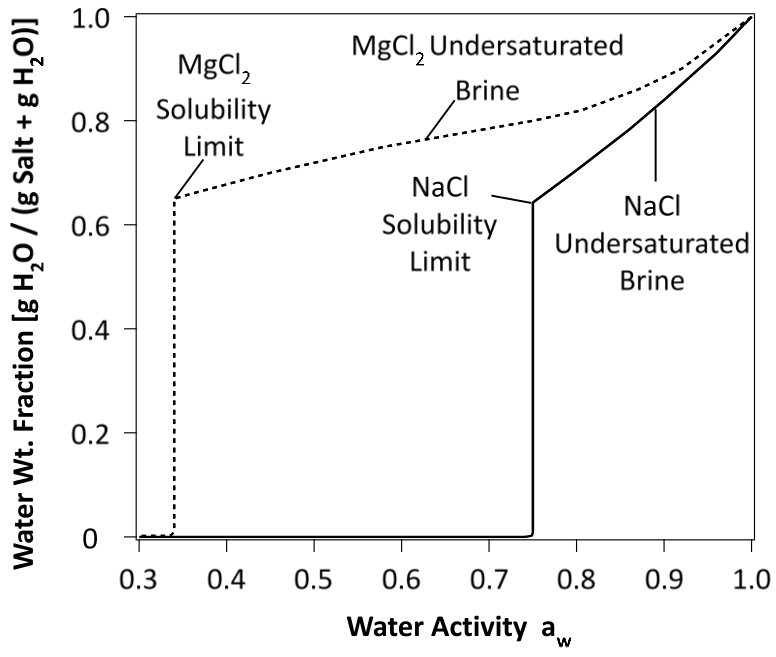

Figure S1.3b: Water adsorption branch isotherm at 25C for $CaCl_2$

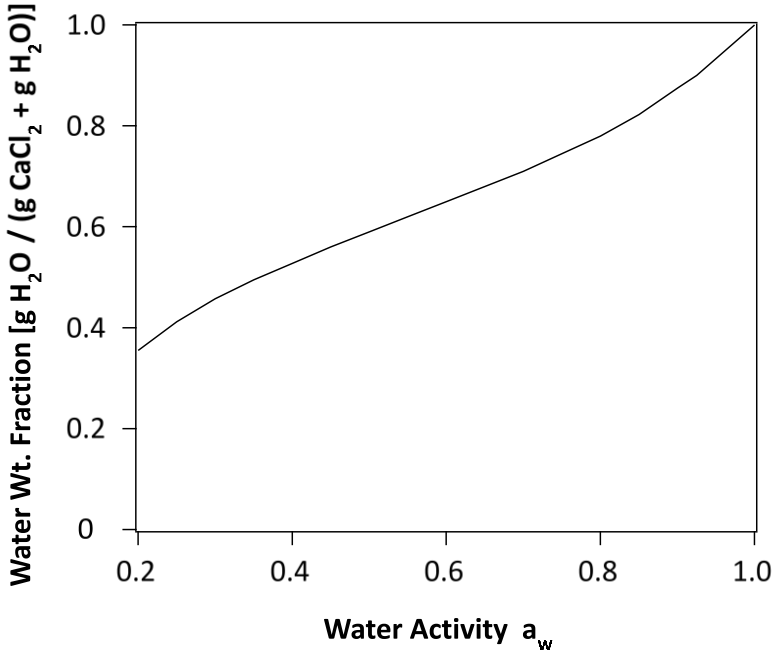

the water content abruptly rises are approximately 0.33 for $MgCl_2$ and about 0.75 for NaCl. The solubility limit has very little temperature dependence changing by less than 2% in a temperature range from 10C to 50C. As such water sorption isotherms for these salts are very similar in the temperature range from 10C to 50C. A consequence of this is that the lowest water activity that can be achieved with $MgCl_2$ addition is ~0.33 and the lowest water activity that can be achieved with NaCl addition is, ~0.75.

Other examples of salts with this saturation behavior are KCl (a_w at saturation about 0.85), LiCl (a_w at saturation about 0.11), K_2CO_3 (a_w at saturation about 0.44). $CaCl_2$, a common salt used for road de-icing, can be used to lower water activity below about 0.2, however its behavior is somewhat more complex because it is extremely hydroscopic. Figure S1.3b shows the adsorption branch isotherm for $CaCl_2$ that has been inferred from data in the literature [24, 25, 26]. Incorporating a sufficient quantity of salt capable of reducing a_w below 0.6 provides a way of lowering water activity for the most assured long term biomass storage. These salts would include $CaCl_2$, $MgCl_2$, K_2CO_3 and LiCl. NaCl on it's own cannot reduce a_w below ~0.75. Nonetheless with further studies NaCl may become a preferred option.

Together the salt and biomass isotherms allow one to compute the minimum amount of salt required to maintain a desired water activity in the dry tomb structure. For example, the amount of $MgCl_2$ salt needed to dry a tonne of very wet miscanthus containing 20wt.% water would be

Figure S1.3c: Mass ratio of $CaCl_2$ salt to dry miscanthus versus mass ratio of total water contained in the biolandfill to dry miscanthus. Lines shown set the amount of salt needed to lower water activity to 0.6, 0.4 or 0.2.

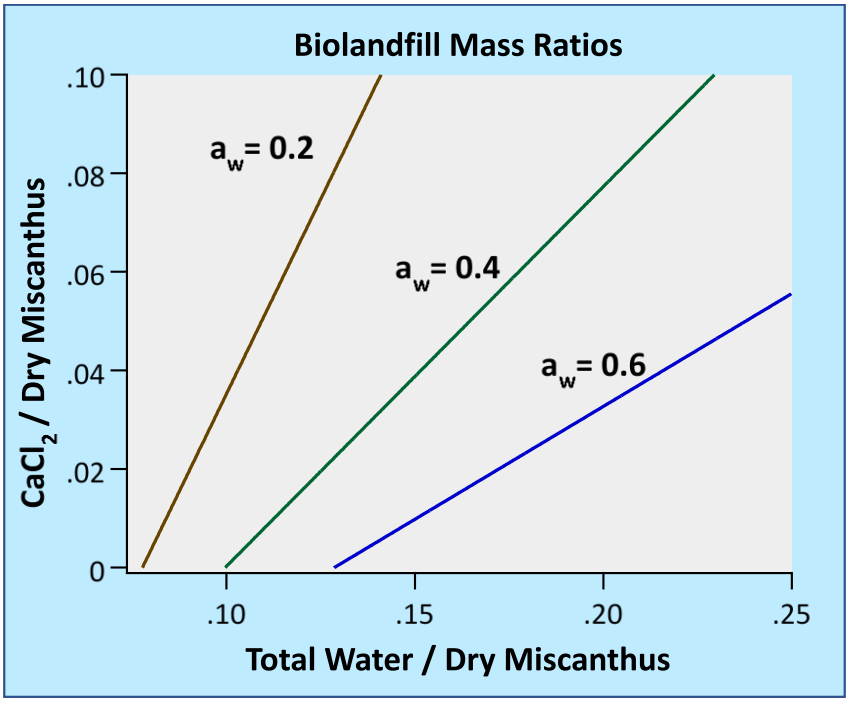

0.036 tonne of dry $MgCl_2$ salt if the final equilibrium target water activity was 0.6. The amount of salt required can be lowered by drying the biomass. For example, if miscanthus was dried to a water content of 15wt.% the amount of dry $MgCl_2$ salt needed to achieve a water activity a_w of 0.6 is reduced to 0.016tonne of $MgCl_2$ per tonne of dry miscanthus. If the miscanthus is dried to a water content of ~12wt% then no salt is needed to achieve a water activity of 0.6.

In a similar manner the miscanthus isotherm in Figure S1.2a and the $CaCl_2$ isotherm in Figure S1.3b were used to calculate mass ratios of {$CaCl_2$ salt /dry miscanthus} and {total water within the biolandfill / dry miscanthus} needed to obtain equilibrium water activities of 0.2, 0.4, and 0.6. Figure S1.3c graphically shows results of these calculations. In these calculations total water is all water in the region where salt is added. If salt is used in a spot treatment in a region where water has seeped through the seam of a tarp, the total water would include water sorbed in the dried biomass as well as any rainwater that wound up being incorporated into dried biomass within the region. If salt is used to mitigate diffusion of water through transport barriers forming the dry tomb structure, then total water would include water sorbed in the dry biomass in a region near the dry tomb boundary as well as water that is expected to permeate through the water transport barriers. If salt is used to set a water activity throughout the entire biolandfill then the region of

interest is the entire dry tomb structure. Within this region the total water is the sum of water sorbed in all of the sequestered biomass along with the amount of rainwater incorporated during construction and ground water diffusing (through the transport barriers) during long term sequestration.

Inspecting Figure S1.3c it is seen that to obtain a water activity of 0.6 in a region that is expected to have 0.2 tonne of water per dry tonne of miscanthus requires 0.033 tonne of $CaCl_2$ salt per tonne of dry miscanthus. This is an example of an extremely wet region since it is planned to dry the miscanthus to a water level below ~12wt.% and to arrive at this high water level, 0.08 tonne of rainwater or groundwater per tonne of dry miscanthus (~8wt.%) would have had to have been incorporated into this region. The graph in Figure S1.3c shows that a dryer region with 0.15 tonne of water per tonne of dry miscanthus would require 0.01tonne of $CaCl_2$ salt per tonne of dry miscanthus to achieve the same water activity of 0.6.

When $CaCl_2$ is used, current cost is not a very important issue in deciding whether to use it in spot treatments to mitigate rainwater invasion, or to use it near the dry tomb boundary to mitigate groundwater invasion or to use it throughout the volume of the biolandfill to reduce the amount of thermal biomass drying required. For treatments with the same $CaCl_2$ wt.% per tonne of biomass, the total amount of $CaCl_2$ used when it is dispersed throughout the biolandfill is 50 to 100 fold greater than when it is used in spot treating and for protection in regions close to the water transport barriers. When a small amount of $CaCl_2$ is used the biomass must be dryer; slightly increasing costs. The most important factor in deciding between treatment scenarios with smaller amounts or larger amounts of $CaCl_2$ is the rapidity and scale at which Agro-Sequestration is deployed setting the fraction of worldwide $CaCl_2$ production needed. Currently the worldwide $CaCl_2$ market is ~4.5million tonnes and is expected to grow to 5.7million metric tonnes by 2029 [27]. If a quarter of current world production was used for Agro-Sequestration in a scenario where it is used for spot treatment of rainwater and to mitigate possible groundwater invasion, we estimate that this supply would be large enough for Agro-Sequestration to offset 20gigatonnes of CO_2 emissions per year. In a much more conservative scenario where $CaCl_2$ is used throughout the landfill to dry biomass at a treatment rate of 0.01 tonne of $CaCl_2$ salt per tonne dry biomass, only ~0.2gigatonnes of CO_2 emissions could be offset per year without dramatically increasing $CaCl_2$ production. In this

conservative scenario which uses large amounts of $CaCl_2$, world production would have to be expanded approximately 10 fold to offset 20gigatonnes of CO_2 emissions per year.

Some increase in production of $CaCl_2$ could come from geological deposits [28], however if a significant production increase were required it would have to come from an expansion of production from chemical reactions. The method currently favored to produce $CaCl_2$ from reaction of calcium carbonate with hydrochloric acid would be limited by HCl availability if world $CaCl_2$ production were significantly expanded. Production of $CaCl_2$ using the Solvay process would not be reagent limited and could in principle be used to expand world production. The Solvay process [29] reacts calcium carbonate ($CaCO_3$) with NaCl to produce $CaCl_2$ and sodium carbonate (Na_2CO_3). Vast expansion of production capacity would produce a world excess of sodium carbonate and we estimate that the cost of $CaCl_2$ would have to approximately triple to make the capacity increase economical. However, it is not clear that such expansion is necessary because sufficient drying of biomass along with spot treatment to mitigate rainwater and groundwater invasion is expected to protect the dryness level. In the most extreme scenario, no salt is added and the biomass is even more thoroughly dried. In the end final decisions around which scenario to implement to obtain a sequestered biomass activity of 0.6 will depend on tradeoffs between operational, regulatory and economic factors.

Calcined gypsum is another type of salt that can be used to lower water activity below 0.6 [30]. Calcined gypsum ($CaSO_4$) is a neutral salt of a strong acid (SO_4^{2-}) and base (Ca_2^{+}) that will act as a sorbent. Gypsum ($CaSO_4\ 2H_2O$) is available on an extremely large industrial scale (~150×10^6 tonne/year) and can be dehydrated at a reasonable price (~$40 / tonne). Also, it is not reagent limited if more production were required. At a water activity of 0.6 its sorption capacity is ~1/8 that of $CaCl_2$. As such significantly larger quantities of this desiccant are required which is in part offset by its relatively low price which is 1/4 of $CaCl_2$. As such it is a potential candidate that will add some cost and volume to the biolandfill. In scenarios where Agro-Sequestration offsets a modest amount of CO_2 emissions per year (for example 2gigatonnes) and bioilandfills with water activities below 0.6 are constructed with large salt contents (8wt% $CaSO_4$), calcined gypsum would be a competitive candidate requiring ~50% of current world production. In scenarios involving smaller amounts (such as spot treatments for rainfall and protection against

diffusional transport of groundwater into the dry tomb structure) calcined gypsum is a strong candidate.

If as anticipated future studies show that a water activity of 0.75 is sufficient for long term biomass sequestration, then NaCl could be used. World Production of NaCl is ~280million tonnes [31] approximately 60 times larger than $CaCl_2$ with approximately half the cost per tonne. With this more abundant and less expensive resource scenarios that rely on drying a significant fraction of biomass with salt become less disruptive. Even in a scenario where biomass sufficient to offset 20gigatonnes of CO_2 is treated with 1wt.% NaCl, the required salt would only account for 40% of current world production. Because of the abundance of dry salt deposits and saline sources, we estimate that this amount of salt could gradually be brought to market with a ~10-20% price increase. Spot treatment mitigating rainwater and ground water would not significantly perturb todays NaCl market.

1.4 Problems With Biomass Preservation In Other Environments.

When photosynthetically generated biomass reaches the end of its life cycle it begins to degrade in a wet aerobic environment with a significant portion of its carbon being released as CO_2 and in a few cases a small portion as methane. In wet aerobic environments a wide variety of insects, microorganisms and fungi can participate in the degradation and CO_2 is the predominant gaseous product, however termites and fungi can produce CH_4 emissions [32]. Rate of degradation and the chemistry is highly dependent on the biomass type and local environment. Only recently has the contribution of microorganisms and insects to global forest deadwood decomposition in wet aerobic environments been quantified along with the total carbon released globally from deadwood [33]. A full comparison with Agro-Sequestration, which is aimed at retaining ~100% of the carbon is complex. The long delay in the greenhouse gas release from decaying biomass such as trees which is set by the biomass life expectancy, and the rate, and extent of decay. As such a full comparison with aerobically decaying biomass which releases greenhouse gases is beyond the scope of this paper, nonetheless it is reasonable to state that from a long-term (100+ years) perspective; reforestation and afforestation will lead to significant future emissions of

greenhouse gases from decaying timber and will not be anywhere near as carbon negative as Agro-Sequestration.

In wet anaerobic environments biomass degradation produces significant quantities of methane that is formed primarily through fermentation fed methanogenesis [34, 35, 36]. This formation of high methane content biogas in anaerobic environments is mediated by complex communities of microorganisms that participate in a multi-step cooperative decomposition pathway. Water activities below 0.6 are expected to suppress the growth of these microorganisms by limiting water transport across cell walls shutting down growth of the microorganisms and hence anaerobic decomposition pathways. The exact limit needed to suppress microorganism growth in dark anaerobic environments has not been experimentally verified and there is a significant possibility that a water activity of 0.75 will suppress microorganism growth.

The asymptotic amount of degradation and amounts of methane generation depend on the type of biomass. Wet (a_w>0.8) anaerobic digesters commercially produce methane from several agricultural wastes. Biomass containing high quantities of lignin (such as wood) is known to be very resistant to wet anaerobic biodegradation and early assessments indicated that even with a wood feedstock there could be significant evolution of greenhouse gases [37,38]. There has been considerable uncertainty about the amount of gas evolved from anaerobic wood decomposition in environments with partial water saturation as well as "waterlogged"). Owing to biodegradable resistant lignin, these moist sequestrations only receive a fractional credit relative to dry Agro-Sequestration.

Empirical support for the idea that wet anaerobic environments can preserve wood was taken from the physical appearance of wooden artifacts preserved for millenia to millions of years [39] in waterlogged or wet impermeable (clay sealed) anaerobic environments. These preservations are often referred to as mummified wood [40] and although it loses much of its carbon, it retains much of its physical appearance [41]. This preservation of physical appearance is due to the degradation resistance of the lignin component, 20-40%, in wood. Unfortunately the cellulosic carbohydrate components degrade more readily [42,43] to produce CO_2 and CH_4. This leads to only a fractional sequestration credit relative to dry Agro-Sequestration.

Rates of degradation and greenhouse gas evolution is dependent on the temperature of the environment in which the wood is mummified. At temperatures near or at freezing, microbial activity slows down and wood as well as other biomasses can exhibit preservation without significant chemical alteration. Unfortunately this will not be the subsurface temperature in agriculturally productive regions and dryness would have to be used to suppress microbial activity and greenhouse gas generation.

1.5 Comparison of Dry Biomass Storage (Agro-Sequestration) With Other Technologies That Photosynthetically Capture Carbon.

Some of the least expensive near-term answers to greenhouse emissions that are being implemented are reforestation and afforestation. In SI Section 1.4 it was shown that in the long term (100+ years) these options will lead to significant future emissions of greenhouse gases from decaying timber and will not be anywhere near as carbon negative as Agro-Sequestration.

Simply burying dried biomass and even dried woody biomass without adequate protection from groundwater invasion would lead to significant greenhouse gas evolution (see SI Section 1.4), although there would be some partial sequestration credit for wood, owing to the higher lignin concentration. Placing biomass in a biolandfill without adequate drying is also expected to lead to greenhouse gas evolution because water activity in the "wet" biomass will support the growth of anerobic microorganisms (see SI Section 1.4).

Bio chars produced from biomass are being promoted as a carbon sink that can improve soil fertility [44]. The carbonaceous product is produced using torrefaction [45] or pyrolysis [46]. Both of these processes require significant investment in chemical processing equipment and to obtain carbon negativity, methane produced in these oxygen starved thermochemical conversion processes must be dealt with. Mitigating methane emissions requires separate processing equipment and to obtain carbon negativity approaching Agro-Sequestration all of the resulting fugitive CO_2 emissions must be captured and sequestered. All of these steps and associated equipment add expenses and costs that are far in excess of Agro-Sequestration.

Second generation biofuels derived from lignocellulosic crops photosynthetically capture CO_2 and have the potential to offset a significant fraction of the world's CO_2 emissions. To date there have been significant problems in their deployment to a large degree associated with high production costs [47] and as such it is uncertain whether a large-scale second-generation biofuel economy will develop. Third generation biofuels produced from algae currently have been significantly more expensive [48]. Apart from high costs our calculations which are in general agreement with those of Amelse and Behrens [19] indicate that, from a land used and energy perspective, it is always more efficient to bury biomass, rather than to process it into liquid fuel. For a simplistic analysis we note that lignocellulosic biomass contains oxygen which must be removed by forming CO_2 to make hydrocarbon fuel. Balancing the chemical equation for converting the carbohydrate like portion to liquid hydrocarbons, about 40% of the biomass carbon ends up, not in the final hydrocarbon fuel, but as CO_2 or other waste products [49] that need to be sequestered. Furthermore, the lignocellulosic biomass processing plant is at best ~80% energy efficient. By comparison the carbon efficiency of Agro-Sequestration is approximately twice as large. This assessment is further supported by comparison with one of the IPCC integrated assessment models for a large biofuel economy (SSP5 - RCP1.9) [50]. Biofuel production in this model appears to offset 15 to 20gigatonne/year of CO_2 emissions in the year 2100 from growth of biomass on 7.6×10^6 km^2 of land. Sequestering 20gigatonne of CO_2 equivalent per year with Agro-Sequestration using our base case carbon contents and crops yield would require agricultural production from 4.8×10^6 km^2. Land requirements for Agro-Sequestration, per unit CO_2 offset, appears to be 1/2 to 2/3 of that for biofuel production in the IPCC SSP5 – RCP 1.9 scenario.

2. Dry Biolandfill Technology

The salted biomass stored in the biolandfill is a biomass salt composite encased in a dry tomb structure formed by top and bottom seals that act as water transport barriers. These barriers completely surround the biomass salt composite preventing ingress of ground water keeping the biomass dry. Their function is the opposite of water transport barriers in conventional municipal and toxic waste landfills. In conventional municipal and toxic waste landfills water transport barriers are used to prevent the contamination of ground waters from outward transport of polluted waters contained in the landfill as opposed to preventing inward transport of ground water into a dry biomass.

A schematic cross section of such a dry tomb biolandfill containing dried compressed salted biomass is shown in Figure S2.a. The biolandfill design is one of many possible designs and is based on best practices for landfills [51, 52] with some notable enhancements. The upper surface of the biolandfill is covered with a vegetative layer (phytocapping) to prevent erosion. Ultra-low permeability bottom and top seal structures contain multiple protective layers as well as two nested polyethylene geomembrane water diffusion barriers separated by a spacer structure shown at the bottom of Figure S2.a. This nested dual water diffusion barrier structure eliminates the effect of pinholes or defects in polyethylene geomembranes. Pinholes and /or defects will occur very infrequently and the probability of pinholes or defects lining up in this nested structure is infinitesimal. The protective layers and spacer structure in the top and bottom seals contain multiple layers that incorporate geotextiles, geocomposites, clay or geosynthetic clay layers as well as soil. Schematic cross sections of the top and bottom seals showing one design for layering in the spacer as well as top and bottom protective layers is shown in Figure S2.b (bottom seal structure) and Figure S2.c (top seal structure). The geosynthetic clay layers in the spacer structure provide an extra degree of protection from water intrusion. The geosynthetic clay layers are thin enough so they will not crack if the clay significantly dehydrates and will swell to shut down water intrusion, sealing any pinholes or defects. Geotextiles provide mechanical protection and the geonet provides water drainage away from the top surface of the dry tomb. In our design the inner protective layers are geocomposites which offer mechanical protection and also can contain geosynthetic clay to provide even more protection from water intrusion.

Figure S2.a: Cross sectional view of biolandfill showing dry tomb structure sequestering a biomass salt composite. Distance across white gap is ~200m and remainder of drawing is approximately to scale. Biomass salt composite within the dry tomb is kept dry by layered top and bottom seal structures containing nested polyethylene geomembranes that are shown at the bottom of the figure and in more detail in Figure S2.b and S2.c. Seals limit water intrusion to less than 1.75μm per year keeping biomass composite dry for thousands of years.

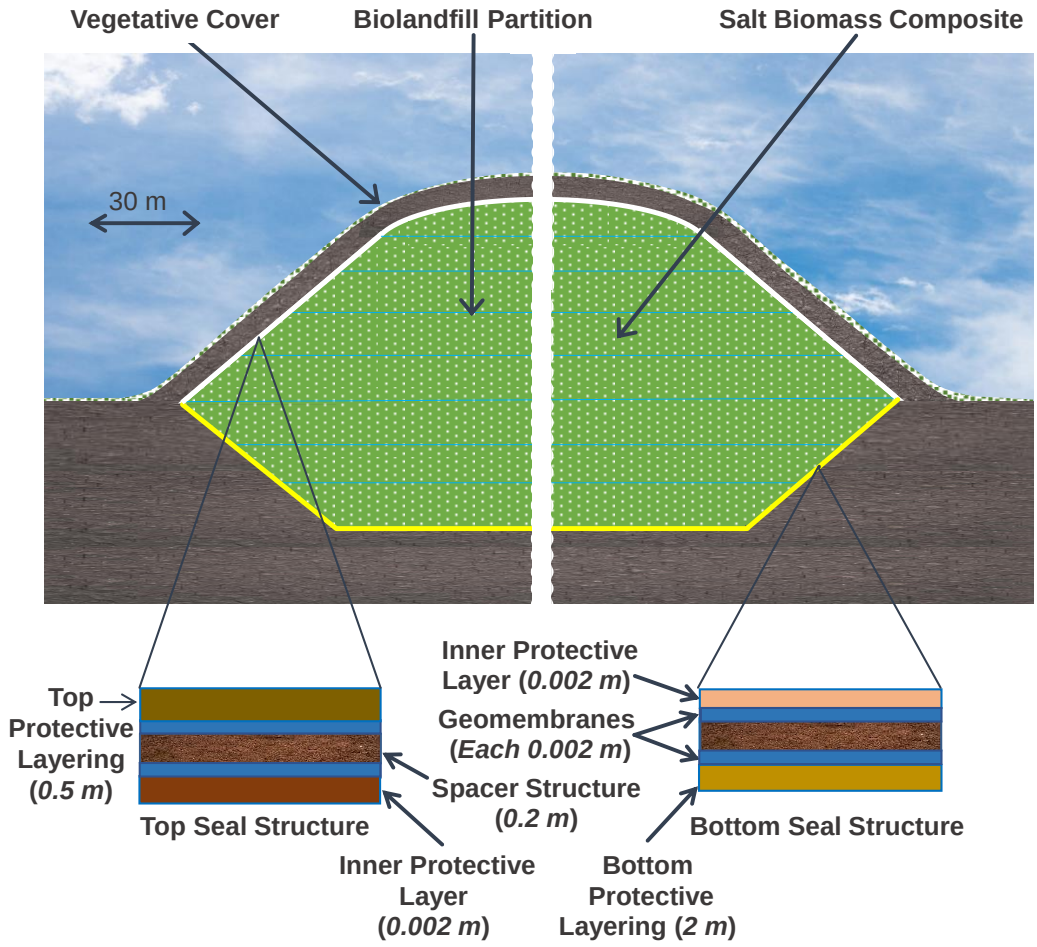

Nested water diffusion barriers in our design are geomembranes formed from 2mm thick polyethylene sheets that are welded together. Currently landfills use similar geomembranes [53, 54] formed from 1-4mm thick low permeability plastic sheets that are welded together. A variety of low permeability plastics have been used including high density polyethylene, low density polyethylene, linear low-density polyethylene and polypropylene. Significant technology

advances have occurred and continue to occur in the formulation of resins to make these geomembranes as well as the ability to weld sheets together and methods that detect imperfections in the welded seams through which water could hydraulically flow. Today GM-17 specifications cover the use of products usually made with 0.91-0.94g/cc low density polyethylene resins and GM-13 specifications cover the use of products usually made with high density polyethylene resins having densities of 0.94g/cc or greater [55, 56]. Historically the higher density polyethylene (GM-13) has had the advantage of greater chemical resistance and the lower density polyethylene (GM-17) has had superior environmental stress crack performance. Significant technology advances have occurred and continue to occur in the formulation of resins to make these geomembranes, as well as the ability to weld sheets together, and methods that detect imperfections in the welded seams through which water could leak. For stability we chose to design with 0.94g/cc geomembranes meeting GM-17 specifications.

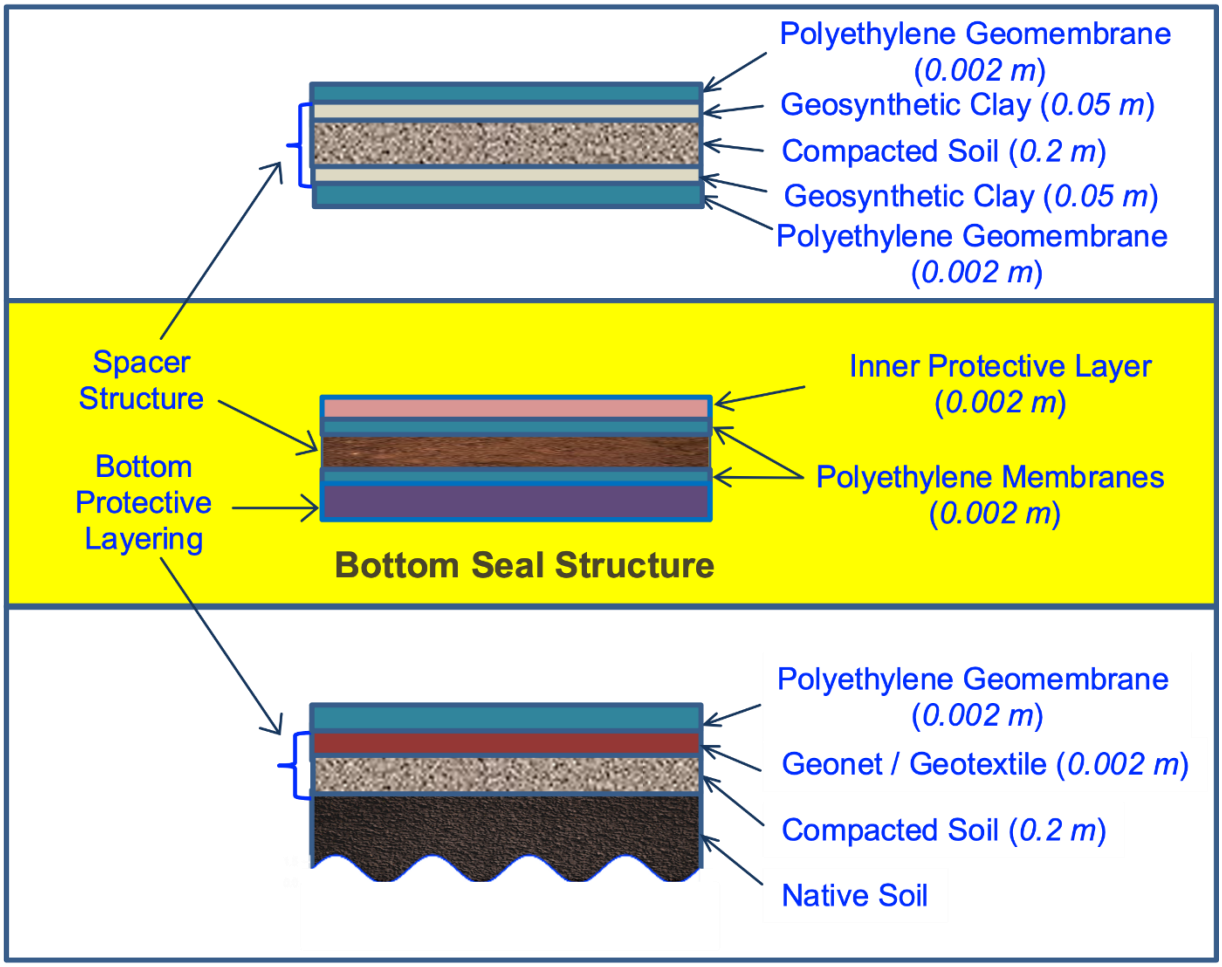

Figure S2.b: Detailed view of bottom seal in the dry tomb structure.

Figure S2.c: Detailed view of top seal in the dry tomb structure.

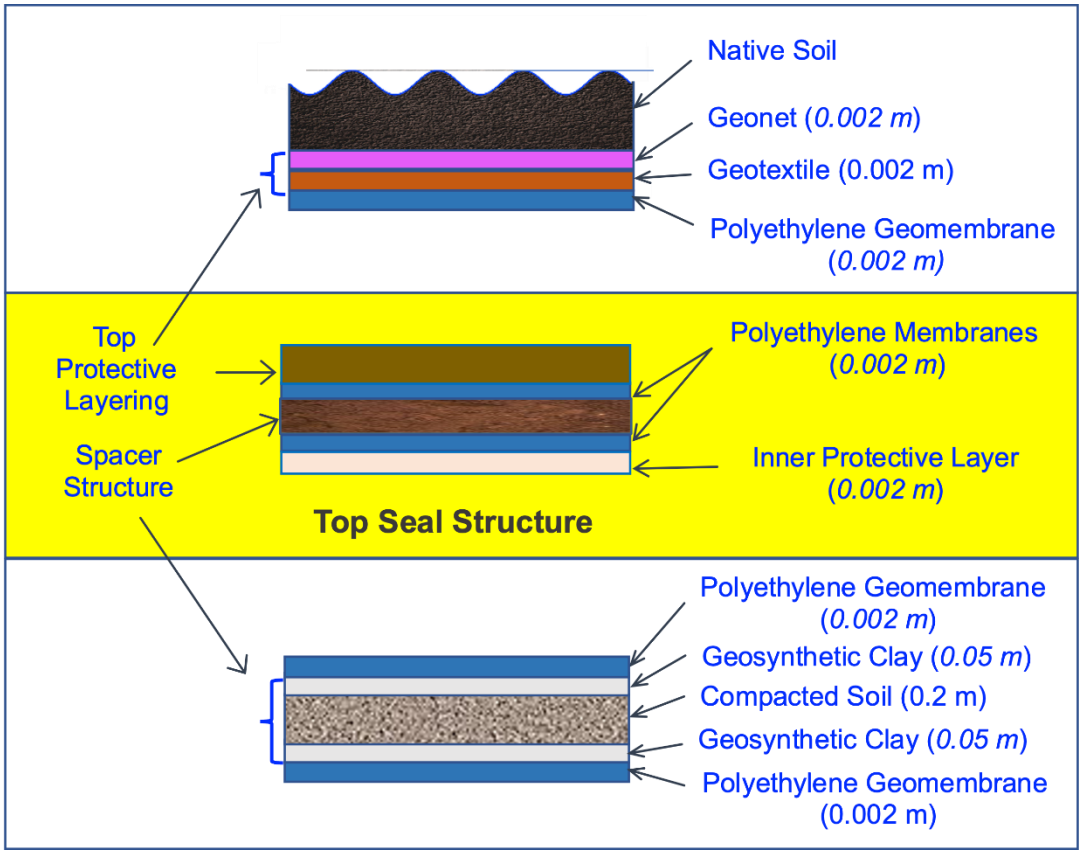

An extreme upper bound on the water flux through such geomembranes can be determined from membrane permeation rates of saturated water vapor (or equivalently 100% relative humidity) across polyethylene sheets of known thickness to a dry side (~0% relative humidity). Because polyethylene sheets are commercially used as vapor and moisture barriers in construction and packaging industries there are a large number of measurements of the Water Vapor Transmission Rate (WVTR) at high relative humidity and it is a specification quoted for many commercial product offerings [57]. Some measurements of the WVTR are done with feeds at 100% relative humidity and we chose to use a set of measurements at 38C for an 89μm thick, 0.94g/cc film [58]. Scaling this data set to a 2mm thick film the permeation from liquid water would deliver an amount in one year equivalent to a 30μm thick water film on the surface of the geomembrane. For two geomembranes the water delivery rate would be less than half this amount (15μm). This extreme gradient of water activity driving permeation through a 2mm thick

geomembrane would not occur in an actual biolandfill. Accounting for geometry and composition of the spacer layer and transport into the biomass salt composite, the delivery rate is expected to be more than a factor of 9 less than this extreme upper limit (i.e. a 1.75μm thick water film per year). A more extensive discussion of water transport across the geomembranes is presented in SI Section 7 along with supporting calculations.

Water originally in the sequestered biomass salt composite within the dry tomb can safely contain an amount of water that is more than 400 times greater than the quantity of water expected to permeate through the top and bottom seals in 1,000years (SI Section 7). As such it is important to dry the biomass as much as practical before sequestering it in the dry tomb structure. Depending on biomass source, water content in biomass arriving at the biolandfill can range from ~10wt% to more than 50wt% with the highest water content in green wood biomass. For high water content biomass most of the water is located in macropores and can be removed by air drying during storage. In general, harvested biomass will have to be stored for a period of time at the biolandfill site and by properly constructing storage it is possible to air dry the biomass. More strongly sorbed water left after air drying is generally in a range from 10wt.% to 20wt.% and in most scenarios a heated drying method is employed to lower water content. There is an optimization in any heated drying process between cost (capital and operating) of heated drying and the amount of salt needed to reduce water activity in the biomass salt composite. Depending on biomass source the optimized target water content for the heated drying processes is a biomass water content of 5% to 15%. To facilitate the biomass handling and aid in the kinetics of drying, biomass is ideally chopped into millimeter to centimeter sized pieces before drying. A few examples of methods for drying the chopped biomass are belt dryers, tunnel dryers, conveyor dryers, rotary dryers, screw conveyed dryers, and fluidized bed dryers.

To improve economics and help limit water activity, dried chopped biomass is compacted to relatively high density either in place within the biolandfill or before it is placed into the biolandfill. Chopping improves the ability to dry biomass and also improves the ability to densify it with compaction technologies. Compacted US municipal landfills which do not have chopped fills are reported to have a density in a range from 0.3 to 0.4g/cc [59] while different compaction technologies for biolandfills can increase chopped biomass salt composite densities in a range from

0.65g/cc to 1.5g/cc. Methods that can be used to compact salted biomass in place include techniques that have been used to compact soils, such as dynamic, vibratory, and quasi-static compaction [60, 61, 62]. Dynamic compaction is a ground improvement technique that densifies soils and fill materials by using a drop weight. The drop-weights typically range from 5 to 40tonnes, and the drop heights typically range from 10 to 30 meters, and sometimes more [63]. Vibratory compaction applies a stress to soil or fill materials repeatedly and rapidly via a mechanically driven plate or hammer [62]. Often this is combined with quasi-static compaction methods such as rolling compaction. Quasi-static compaction techniques are commonly used in municipal landfills and apply stress to the soil or fill material at a slower rate by rolling a heavy cylinder across the surface or by the kneading action of devices such as a 'sheepsfoot' roller [64]. Higher density compression can be achieved with reciprocating ram/piston presses, screw presses, roll presses, and extruders that produce briquettes in the form of bricks, sheets, pellets, or extrudates [65, 66]. This type of machinery can produce compaction pressures of 300 to 3000bar yielding compacted biomass briquettes as well as salt biomass composite briquettes with bulk densities ranging from 0.75 to 1.5g/cc [66, 67].

Besides having higher density fill and lower water content, biolandfills have several notable enhancements when compared to municipal landfills. One such enhancement is the use of secondary and in some instances tertiary water barriers within the dry tomb structure to partition the biomass salt composite. Secondary partitions are shown schematically as light blue lines in the biolandfill cross section shown in Figure S2.a, and provide additional protection to keep biomass dry during construction of the biolandfill as well as during the lifespan of the dry tomb structure. These can be thinner sheets of polyethylene. In some designs the salt biomass composite is plastic wrapped or bagged and in these instances the plastic film encasing the biomass salt composite forms a tertiary water barrier. The most important enhancements are provisions for biolandfill verifiability. Modifications that make the biolandfill verifiable involve installation of piping that allow sampling of gas composition and /or pressure in the landfill from the earth's surface. Monitoring of pressure allows detection of any pressure buildup from biogas generated by biomass degradation. Monitoring of gas composition in the dry tomb structure allows an assessment of water activity as well as detection of any biomass degradation. Over time water activity will thermodynamically equilibrate throughout most of the volume in a sealed dry tomb

structure. This equilibration produces identical activities for water sorbed in the biomass, water sorbed by salt, and water vapor in the gas space. As such sampling the gas space from a dry tomb structure provides a means of measuring water activity. Equivalently, because CO_2 and CH_4 are biomass degradation products, careful monitoring of the gas composition provides an assessment of small amounts of degradation.

There are a wide range of methods that can be used to construct biolandfills. Construction techniques involve a wide variety of engineering and scientific practices such as construction engineering, environmental engineering, geotechnical engineering, materials science, materials engineering, site development and planning, structural engineering, surveying, water resource engineering, chemical and process engineering, analytical chemistry, pedology, agronomy, biology, and civil systems engineering. Only a brief high-level discussion touching on a few of the myriad of possible construction methods will be presented. Methods used to construct biolandfills which have a base above or near the earth's surface will differ from construction methods which have a base well below the earth's surface. Biolandfill construction would begin by preparing a surface on which the bottom water transport barrier or barriers would be installed. If the biolandfill is below the earth's surface this would involve excavation of an open pit structure while for construction at the earth's surface this would primarily involve grading the surface of the land.

Provision needs to be made to drain rainwater from the excavated or graded structures as well as from the biolandfill during construction. In case of salt contamination of runoff water during construction, the water can be purified by reverse osmosis and distillation. One possible provision to handle rainwater is sloping newly exposed soil surfaces so water drains to a spot where it can be pumped or channeled and disposed of. Other methods are diverters, gutters, plastic sheeting, or tarp systems designed to channel rainwater away. Different types of diverters or gutters will be used throughout construction and can be made from earthen structures, plastics, tarps, or sandbags. After excavation or grading, water transport barriers are then installed on the exposed surface of what will become the bottom of a dry tomb structure along with any spacers between these water transport barriers. This step may also involve the instillation of a protective

barrier between the ground and outermost water transport barrier or between the biomass and innermost water transport barrier.

At this point the salted biomass composite can be added into the biolandfill. It is envisioned that biomass would be stored at or near the biolandfill site. Ideally storage would be in a relatively dry condition such as under a tarp or in a warehouse or shed and would be dried and chopped before adding it into the biolandfill being constructed. The way in which it is added depends significantly on how the biomass is compressed as well as how the salt biomass composite is formed. It can be physically stacked in the biolandfill if it is compacted with equipment that chops, dries, and produces composite salt biomass briquettes (potentially plastic wrapping or bagging them), or pure biomass briquettes with a separate salt addition (with potential plastic wrapping or bagging). Similarly compressed dry salt biomass composite bales or pure biomass bales with a separate salt addition can be physically stacked within the biolandfill. In addition, these bales can be plastic wrapped. When compressed biomass with a separate salt addition or compressed salt biomass composites are stacked as briquettes or bales, earthworks may in some instances be constructed to hold them in place, providing an anchoring point for a temporary tarp system, or providing drainage for rainwater, or providing the base for a temporary canopy structure used to protect areas from rain moisture. Potentially these earthwork anchors could occupy 15% of the volume of the finished dry tomb structure and would build up as the height of the stacked salt biomass composite increases. One form of earthwork would be a dike structure or earthen causeways forming channels into which the compressed salt biomass composite is stacked. In addition, these earthworks could be used to compartmentalize regions of the biolandfill with sealed plastic sheeting that acts as secondary water transport barriers.

For mechanical compaction, biomass is dumped as a layer in a portion of the biolandfill and mechanical compaction equipment is run over it in multiple passes to densify it. Salt can be homogeneously mixed with the biomass or added heterogeneously (for example in a thin layer). Construction with this type of compaction can be done with or without earthworks. To keep salt biomass composites dry, temporary tarp systems and / or canopies can be constructed. In addition, plastic sheeting can be installed to seal off areas that are fully compressed. Such sealed plastic sheeting compartmentalizes the biolandfill and provides a secondary water transport barrier.

When the salted biomass rises above the earth's surface to the full height of the dry tomb, the upper water transport barriers are installed along with any spacer structures or additional layers used to protect the inner and outermost water transport barriers. Soil is used to cover the completed dry tomb and water transport barriers. Analytical instrumentation for verification requires piping rising above the biolandfill surface and is completed with instillation of valving.

3. Candidate crops and biomass availability

3.1 Candidate crops

A partial listing of crops that are suitable to produce biomass for Agricultural Carbon Capture and Sequestration is presented in Table S3. Crops in Table S3 are highly productive and have dry biomass yields in a range from 4 to greater than 45 dry tonne/hectare/year. In addition, they are not food crops. As noted in the manuscript many of the candidates are energy crops that were developed for biofuels. Algae is an additional high yield biomass that could be used which does not appear in the table because it requires special growth and harvesting techniques and special drying conditions. Many of the crops shown in Table S3 can be grown on marginal or degraded lands with reduced yields. For some crops such as kudzu and transgenic eucalyptus care must be taken to prevent their spread from the agricultural site because they are invasive. Sections 4 and 5 in the SI present a bottom-up economic analysis for producing biomass for three of the crops listed in Table S3, namely miscanthus, switchgrass and loblolly pine.

3.2 Biomass availability

Many crops suitable for Agro-Sequestration are not good candidates for biofuel production; however using worldwide and regional assessments of the potential to scale-up biomass production for biofuels provides a good starting basis to assess biomass availability for large scale Agro-Sequestration. Worldwide assessments of biomass availability for large scale biofuel production that we considered come from IPCC Shared Socioeconomic Pathway (SSP) and Representative Concentration Pathway scenarios such as SSP1-RCP1.9, SSP2-RCP1.9, and SSP5-RCP1.9 [50].

The largest land use change in this set of models is for SSP5-RCP1.9 where by the year 2100 7.6×10^6 km^2 of land is repurposed for biofuel production. Contributions to land used for biofuel production in these models come predominantly from pastures, forests, and natural lands (grasslands and shrublands). The IPCC has defined many of the impacts (socioeconomic, water, food production,…) coming from such a large change in land use. Such large changes in land use do have significant impacts, however if carbon drawdown is deemed important with difficulty, large changes appear possible. In our scenario where 20gigatonnes of CO_2 emissions are offset by Agro-Sequestration with average crop yields of 22 tonne / hectare and an average of 50wt. % carbon, approximately 2/3 of the land area (4.8×10^6 km^2) is needed compared to the model for SSP5-RCP1.9. This smaller amount of land corresponds to 1/5 of the world's row cropland [68], or 1/15 the land area of all croplands, pastures, and forests [69,70].

To provide regional context for a less aggressive target, we consider in SI Section 8 a detailed material balance for Agro-Sequestration of 500million tonnes /year of biomass with in the United States. This amount of biomass would offset ~925million tonnes of CO_2 emissions per year. This would be an initial defensible target that would not be as disruptive as worldwide sequestration biomass offsetting 20gigatonnes of CO_2 emissions. Context for this target is provided by the DOE's 2016 Billion Ton Report [71]. This report evaluated the potential amount of biomass that could be economically available for new industrial uses in the US and concluded that approximately a billion tons could be made available by 2040 at a price of $60/ ton or less. The report examined price / supply sensitivities and provided a detailed look at exact places where sources could become available. One significant conclusion was that a very large amount of biomass could come very economically from agricultural wastes and for the 500million tonne case in Section 8 we have included production of 100million tonnes of biomass from agricultural wastes.

Table S3: Candidate Biomass Crops:

Classification	Technical Name	Common	References
Herbaceous Grass	Miscanthus	Miscanthus x giganteus, Silvergrass	72, 73
Herbaceous Grass	Panicum virgatum	Switchgrass	74
Herbaceous Grass	Pennisetum purpureum	Elephant Grass Napier Grass, Uganda Grass	75
Herbaceous Grass	Arundo donax	Giant Reed, Indian Grass, Spanish Reed	76, 77
Hybrid	Miscanthus x Sugarcane	Makarikari Grass	78
Nitrogen Fixing	Pueraria	Kudzu, Japanese Arrowroot	79
Nitrogen Fixing	Medicago sativa	Alfalfa	80
Woody	Bambusoideae	Bamboo	81
Short Rotation Coppice	Salix	Common Osier, Basket Willow, Willow	82, 83
Short Rotation Coppice	Populus	Poplar, Hybrid poplar, Eastern Cottonwood	83, 84
Short Rotation	Eucalypteae	Eucalyptus, Gum Tree	84, 85
Hybrid Tree	Transgenic Trees	Transgenic Eucalyptus	86
Tree / Shrub	Acacia	Mimosa, Acacia, Thorntree,	87
Tree	Pinus	Pine, Loblolly Pine	88
Aquatic	Seaweed	Kelp	89
Herbaceous Plant	Agave tequilana	Blue agave, Tequila agave,	90
Herbaceous Plant	Saccharum	Energy Cane, Sugarcane	91

4. Detailed Analysis of Costs for Growth and Sequestration of Miscanthus and Switchgrass

Miscanthus and switchgrass were chosen as models for a detailed techno economic evaluation in part because they have been extensively studied [92, 93, 94, 95, 96, 97, 98, 99, 100, 101, 102, 103, 104, 105, 106, 107] and many economic models for production have been created. Dry biomass yields from fertilized growth of miscanthus is expected to vary from ~9 to ~30 tonne/hectare/year depending on location and ~4 to ~18tonne/hectare/year for switchgrass. After the recent development of the 'Liberty' switchgrass variety it is expected that further advances in breeding will increase yields in the near future for fertilized switchgrass growth to more than 20tonne/hectare/year. Both miscanthus and switchgrass can be grown on marginal lands with crop yields in the lower end of the production spectrum.

4.1 Cost Structure for Establishment and Growth of Miscanthus

An economic model from the Iowa State Extension Service [94] was used as a template to develop a reference case estimate of yearly fertilized miscanthus growth costs. The model includes field preparation for miscanthus starting a year before rhizome planting, weed control in the early stages of growth, fertilization, and changes in crop yield during establishment. The base case model used a dry yield for a mature crop of 22.5tonne/hectare/year and a land charge of US$494/hectare/year which will change depending on the type of land (pasture, row crop, or marginal) and in the United States whether or not it is enrolled in the Conservation Reserve Program.

The Iowa State Extension Service model [94] was modified to

Pre-establishment Cost for Field Preparation	US$/Hectare
Brush Mowing	25
Disking, Tandem	70
Soil Finishing	74
Net Cost of Herbicide Tolerant Crop in Previous Year	185
Winter Cover Crop (Oats)	80
Total Cost Year Before Planting Miscanthus	**434**

Table S4.1a: Miscanthus pre-establishment costs for field preparation in excess of revenue from herbicide tolerant crop and winter oat cover crop in the year before rhizome planting.

account for a silage harvesting method which we think would be preferred. Most preferably the harvest would be in late fall or winter when the crop has dried and many nutrients have returned to the soil (lowering fertilization costs). Also included is a charge for transportation to a local biolandfill. Yearly expenses per acre for the reference model are summarized in Tables S4.1a, S4.1b, S4.1c, and S4.1d. In the base case model, miscanthus pre-establishment costs for field preparation in excess of revenue from a herbicide tolerant crop and a winter oat cover crop in the year before rhizome planting (Table S4.1a) is ~US$430/hectare. Costs during the year in which rhizomes are planted (Table S4.1b - year #1) come to ~US$3,150/hectare. Farming and transportation costs during the next year in which the first harvest is conducted with a yield of 11 dry tonne/hectare (Table S4.1c) are ~US$770/hectare. Farming, mild drying, and transportation costs during the following years in which mature crops are harvested with a yield of 22.5 dry tonne/hectare (Table S4.1d) are US$900/hectare.

Table S4.1b: Miscanthus costs during year number 1 in which rhizomes are planted.

Costs During Year #1 (Rhizome Planting)	US$/Hectare
Land Charge	494
Machinery Operations	
Disking, Tandem	69
Soil Finishing	72
Fertilizer Spreading	12
Spraying Chemicals	37
Rhizome Planter (NEF Planter)	124
Tractor for Planting (250 horsepower)	35
Land Rolling, Post Planting	20
Interest Expense For Machinery	133
Total For Machinery Operations	501
Operating Expenses	
Soil Test	5
Rhizomes	1556
Fertilizer	319
Lime	215
Herbicides	59
Total Operating Expense	2154
Total Cost for Year #1	**3149**

Table S4.1c: Miscanthus costs during year number 2: first harvest (yield= 1/2 of mature crop).

Costs During Year #2 (Yield= 1/2 of Mature Crop)	US$/Hectare
Land Charge	494
Machinery Operations	
Fertilizer Spreading	12
Spraying Chemicals	20
Interest Expense For Machinery	7
Total For Machinery Operations	39
Operating Expenses	
Fertilizer	82
Herbicides	44
Total Operating Expense	126
Harvesting	
Silage Type of Harvesting	86
Transport to Landfill + Some Crop Drying	26
Total Harvesting, Transport, & Drying Expense	112
Total Cost for Year #2 (First Harvest)	**772**

Table S4.1d: Miscanthus costs for year number 3^{+}: harvests of mature crop.

Costs For Year **Number** 3+ (Mature Crop)	US$/Hectare
Land Charge	494
Machinery Operations	
Fertilizer Spreading	12
Interest Expense For Machinery	10
Total For Machinery Operations	22
Operating Expenses	
Fertilizer	163
Total Operating Expense	163
Harvesting	
Silage Type of Harvesting	170
Transport to Landfill + Some Crop Drying	50
Total Harvesting, Transport, & Drying Expense	220
Total Cost for Year #3+ (Mature Crop)	**900**

4.2 Cost Structure for Establishment and Growth of Switchgrass

An economic model from the Iowa State Extension Service [99, 100] was used as a template to develop a base (or reference) case estimate of yearly fertilized switchgrass growth cost. The reference model is based on 'Liberty' switchgrass with a yield of 13.5tonnes per hectare (dry biomass) and a land charge of US$494/hectare/year which will change depending on the type of land (pasture, row crop, or marginal) and in the United States whether or not it is enrolled in the Conservation Reserve Program. The model includes field preparation for switchgrass starting a year before planting, weed control, fertilization, and changes in crop yields during establishment. The Iowa State Extension Service model [99, 100] was modified to account for a silage harvesting method which we think would be preferred. Also included is a charge for mild drying and transportation to a local biolandfill. Yearly expenses per hectare for the base case model are summarized in Tables S4.2a, S4.2b, S4.2c, and S4.2d. In the base case model, switchgrass pre-establishment costs for field preparation in excess of revenue from a herbicide tolerant crop and a winter oat cover crop in the year before planting (Table S4.2a) is ~US$435/hectare. Costs during the year in which switchgrass is planted and a first harvest is conducted with a yield of ~7tonne/hectare come to ~US$865/hectare (Table S4.2b - year #1). Farming and transportation costs during the next year in which there is a second planting and harvest with a yield of 13.75 dry tonne/hectare (Table S4.2c) are ~US$790/hectare. Farming and transportation costs during the following years in which mature crops are harvested with a yield of 13.75dry tonne/hectare (Table S4.2d) are ~US$732/hectare.

Table S4.2a: Switchgrass pre-establishment costs for field preparation in excess of revenue from herbicide tolerant crop and winter oat cover crop in the year before planting.

Pre-establishment Cost for Field Preparation	US$/Hectare
Brush Mowing	25
Disking, Tandem	70
Soil Finishing	74
Net Cost of Herbicide Tolerant Crop in Previous Year	185
Winter Cover Crop (Oats)	80
Total Cost Year Before Planting Switchgrass	**434**

Table S4.2b: Switchgrass costs during year number 1 in which field is planted and first harvest conducted.

Costs During Year #1 (First Planting and Harvest)	US$/Hectare
Land Charge	494
Machinery Operations	
Spraying Chemicals	37
Drilling, grass seed	40
Interest Expense For Machinery	10
Total For Machinery Operations	87
Operating Expenses	
Soil Test	5
Seed Cost (pure live seed)	185
Herbicides	32
Total Operating Expense	222
First Harvest: Yield = ~7 dry tonne / hectare	
Silage type of harvesting	52
Transport to Landfill + Some Crop Drying	9
Total Harvesting and Transport Expense	61
Total Cost for Year #1	**865**

Table S4.2c: Switchgrass costs during year number 2: replanting and second harvest.

Costs During Year #2 (2nd Planting and Harvest)	US$/Hectare
Land Charge	494
Machinery Operations	
Fertilizer Spreading	12
Spraying Chemicals	20
Drilling, grass seed	40
Interest Expense For Machinery	5
Total For Machinery Operations	77
Operating Expenses	
Seed Cost (pure live seed)	20
Fertilizer	64
Herbicides	15
Total Operating Expense	99
Second Harvesting: Yield = 13.5 dry tonne / hectare	
Silage Type of Harvesting	104
Transport to Landfill + Some Crop Drying	19
Total Harvesting and Transport Expense	122
Total Cost for Year #2	**792**

Table S4.2d: Switchgrass costs for year number 3^{+}: harvests of mature crop.

Costs For Year #3+ (Mature Crop)		US$/Hectare
Land Charge		494
Machinery Operations		
	Fertilizer Spreading	12
	Spraying Chemicals	20
	Interest Expense For Machinery	5
	Total For Machinery Operations	37
Operating Expenses		
	Fertilizer	64
	Herbicides	15
	Total Operating Expense	79
Harvesting	*Yield = 13.5 dry tonne / hectare*	
	Silage Type of Harvesting	104
	Transport to Landfill + Some Crop Drying	19
	Total Harvesting and Transport Expense	122
Total Cost for Year #3+		**732**

4.3 Technology for anaerobic landfills and cost estimates

4.3a *Technical basis for biolandfill design*

Costs for biolandfills will vary significantly depending on siting and the technology used to construct them. For a base case (or reference) biolandfill construction and closure cost estimate we used a design based on best practices for municipal landfills [108, 109, 110, 111, 112, 113] and an overview of our design is shown schematically in Figures S1.a. The design has top and bottom seals that form a dry tomb structure and details of the layers in the top and bottom seals are shown in Figures S1.b and S1.c. To mitigate water permeation the reference design uses 2mm thick ~0.94g/cc linear low density polyethylene sheets welded together to form a geomembrane. Such geomembranes are used in conventional landfills. To further reduce water invasion two such geomembranes are nested within the top and bottom seals that form the dry tomb structure as shown in Figures S1.b and S1.c, limiting any water leakage at defects. The spacer layer between the nested geomembranes is also shown in Figures S1.b and S1.c and incorporates geosynthetic

clay layers and a compacted rock free soil layer. The reference design also incorporates provisions to make the biolandfill verifiable. Excavation depth used in our base model was ~12meters and the biolandfill is filled to a height of ~18.5meters above the earth's surface giving a total fill height of 30.5meters. Including capping layers, the reference biolandfill would rise 27.5meters above the earth's surface.

4.3b *Technology to dry, compact, and sequester crops in the biolandfill*

Operations at a biolandfill differ from those at municipal landfills. This section provides an overview of our operational model for switchgrass and miscanthus. In the base case model, a chopped crop arrives at a local biolandfill after silage type harvesting, and is compressed using conventional machinery into storable bales with a density in the range of 0.1-0.25g/cc. If the crop arrives too wet (notionally >15wt. % H_2O) it is dried before baling. These bales are then stacked and stored in a warehouse, shed, or under a tarp until they can be processed over the next 10 months. Steps may be taken during storage to further reduce water content such as exposing them to solar radiation during dry hot days. Before placing the biomass in the biolandfill it is dried using a rotary drier to 8-10wt.% water. In a very conservative base case design, all the product is composited with 2.5wt.% $CaCl_2$. In other designs that use less $CaCl_2$, it is only applied in spot treatments mitigating rainwater and potential ground water invasion. For volumetric efficiency the biomass salt composite is compacted with a combination of quasi-static and dynamic compaction. Initially quasi-static compaction is done using a 'sheepsfoot' roller and after a sufficiently thick layer has been put in place dynamic compaction is done using a weight drop. Measured compaction curves [114, 115, 116, 117] for small particulate (i.e. chopped) miscanthus and switchgrass require pressures ranging from ~550-950atmospheres to achieve compressed biomass densities ranging from 0.5g/cc to 1.1g/cc. From the combination of quasi-static and dynamic compaction fill densities of ~0.85g/cc or greater are expected. At this density (0.85g/cc) each hectare of biolandfill would sequester ~250,000tonnes of dry biomass. One hectare of biolandfill corresponds to the yearly production from ~11,000hectares of miscanthus or ~18,500hectares of switchgrass. Filling 16hectares of a biolandfill might ultimately sequester 4,000,000tonnes of biomass/year and service farms within a 30–70kilometer radius, offsetting ~7million metric tons of CO_2 emissions annually. Our near-term base case should have

significantly reduced costs for biolandfill operations in later years due to an "experience curve". (See Section 9.)

4.3c *Economic model of biolandfill CAPEX and OPEX for initial miscanthus and switchgrass projects*

In our accounting method, biolandfill construction and closure are CAPEX costs. OPEX costs are associated with biolandfill operations such as drying and compaction.

A large number of economic models have been developed for construction and closure of landfills and we chose to use as a template an updated version of one that was published in three parts in *MSW Management* [118, 119, 120]. Costs for construction of the base of the biolandfill come to ~US$1,730,000/hectare and itemized costs are given in Table 4.3a. Biolandfill closure costs in our model is ~US$800,000/hectare and itemized costs are given in Table 4.3b. As might be expected operational costs are greater than the ~US$3.25/tonne to ~US$6.75/tonne associated with conventional landfills. Operational costs associated with dry storage, drying, filling, compaction, protection from rain and other landfill operations are presented in Table 4.3c for early demonstration projects. Dry storage is calculated to be US$6.60/tonne of crop for ~1tonne bales placed on pallets and covered with tarps. Approximately one third of the storage cost is

Table S4.3a: Construction cost for biolandfill base structure.

Construction Costs	US$/Hectare
Land Acquisition and Permitting	123,500
Clear and Grub	7,400
Site Survey	17,300
Excavation	345,800
Perimeter Berm	37,050
Geomembranes	209,950
Geocomposites and Geotextiles	185,250
Granular Soil, Clay, Sand and Gravel	172,900
Piping	37,050
Rain Water Protection	148,200
Rotary Dryer	247,000
QA/QC	197,600
TOTAL	**1,729,000**

associated with tarps, another third is associated with pallets, ground conditioning, and pallet handling and the final third is associated with baling costs.

Table S4.3b: Biolandfill closure cost.

Biolandfill Closure Costs	US$/Hectare
Final Grade Survey	9,900
Geomembranes	209,950
Geocomposites, Geonet and Geotextiles	185,250
Granular Soil, Clay, Sand and Gravel	148,200
Vegetative Soil & Planting Phytocap	49,400
Runoff System	14,800
QA/QC	185,250
TOTAL	**802,750**

In a base case model heated electric drying is used to reduce biomass moisture content by 6wt% (6 points) to an average moisture content of 6-10wt.%.

About 90% of the OPEX cost associated with heated biomass drying in our design case is for electric energy. Electricity was priced at US$0.12/kwhr costing US$7.70/tonne of biomass dried by 6 points in a heat integrated electric dryer. This corresponds to an electric energy usage, [121], of ~39kilojoule per kilogram of biomass for each point of drying, or equivalently 62kilojoule/mole of water removed, which is ~20% larger energy than the known minimum for water desorption, [122]. Many of the current generation electric driers are half as efficient [121], (not heat integrated). Medium temperature natural gas and propane fired driers currently require an energy input of 67kilojoule/mole of water removed while high temperature natural gas and propane fired driers require an energy input of 75kilojoule/mole of water removed [123]. At a cost of $2.70/gallon of propane, the energy cost for drying with propane is almost identical to the US$0.12/kwhr cost for electric drying.

A combination of quasistatic compaction and dynamic compaction are used to compress the fill to an average density of 0.85g/cc. Cost of the compaction is estimated to be US$6.60/tonne and cost of tarping and other rainwater protection is estimated to be US$5.50/tonne. In total the OPEX costs come to US$33/tonne of dry biomass and are expected to decrease if Agro-Sequestration becomes widely adopted.

Table S4.3c: Estimated biolandfill operating costs during construction (US$/tonne of crop sequestered) for early demonstration project.

Biolandfill Operating Cost	US$/Tonne of Biomass
Dry Storage	6.60
Electricity for Drying by 6 Points*	7.70
Salt	4.40
Dynamic and Quasi-static Compression	6.60
Rain Water Protection	5.50
Landfill Handling Operations	2.20
TOTAL	33.00

In our base case model electric energy consumption for drying biomass by one point (1 wt.%) is ~10kilowatt hour/tonne and at $0.12/kilowatt hour the electricity cost comes to ~$1.30/point/tonne of biomass. By comparison for each tonne of biomass ~0.004tonnes of $CaCl_2$ are required to dry by one point at a water activity of 0.6. and 0.007tonnes of $CaCl_2$ are required to dry by one point at a water activity of 0.4. If $CaCl_2$ is purchased at a cost of $175/tonne then the cost of drying by one point, at a water activity of 0.6, is ~$0.70, while the cost of drying by one point, at a water activity of 0.4, is ~$1.10. In these scenarios it is cheaper to dry with $CaCl_2$ compared to heated drying. If a water activity of 0.75 is acceptable, then NaCl can be used. The cost of NaCl is less than half the cost of $CaCl_2$ and salt drying cost would be reduced by more than a factor of two.

If electricity was purchased from the grid, greenhouse gas emissions from electric energy generation would be 0.004tonne of CO_2 for drying 1 tonne of biomass by 1 point with heat integrated electric drying. Drying by 6 points emits 1.3% the amount of CO_2 captured by the biomass if the electricity came from the grid. As more renewable electric energy becomes available this number will significantly decrease. If fired propane drying was used greenhouse emissions would be ~0.0028tonne of CO_2 for drying 1 tonne of biomass by 1 point. Drying by 6 points emits ~0.9% the amount of CO_2 captured by the biomass.

4.4 Summary of base case economics for growth and stable sequestration of miscanthus and switchgrass crops in biolandfills.

To calculate a direct cost for CO_2 capture a discounted cash flow (DCF) analysis was applied to the cost structures in the base case models for miscanthus farming, switchgrass farming, and biolandfills that were presented in SI Sections 4.1, 4.2, and 4.3 respectively. Discounted cash flow (DCF) is commonly used for economic analyses that honor the time value of money and compounded returns, providing a way to account for establishment costs for the crops and biolandfills. In the model, the crop and biolandfill establishment required two years and the project lifetime was 18 years for miscanthus and 14 years for switchgrass. A 6% return rate was used for the base case analysis with a 2% inflation rate and a 20% tax rate. Costs per hectare of farmland and returns were computed yearly over the life of the project with ~9×10^{-5}hectare/year of biolandfill required to support a hectare of miscanthus farming and 5.5×10^{-5}hectare/year of biolandfill required to support a hectare of switchgrass farming.

Table S4.4a: Base case Agro-Sequestration (Agro CCS) cost summary for miscanthus. Cost of sequestered carbon is computed from the sequestered miscanthus price using 48wt.% carbon in dry miscanthus. All costs of sequestered CO_2 employ the molecular weight ratio 12/44 and are rounded to nearest dollar.

Agro CCS Base Case For Miscanthus	Sequestered Miscanthus Cost US$/Tonne	Cost of Sequestered Carbon US$/Tonne of C	CO_2 Capture Cost Equivalent US$/Tonne of CO_2
Landfill OPEX	33	69	19
Landfill CAPEX	15	32	9
Establishment	10	21	6
Farmland	22	46	13
Farming Cost Post Establishment	18	38	10
Total Sequestration Cost	98	205	56

The CO_2 cost for stable sequestration of carbon fixed by miscanthus comes to US$56/metric ton of CO_2. A detailed breakdown of this cost structure for Agro-Sequestration of miscanthus is shown in Table 4.4a. The CO_2 cost for stable sequestration of carbon fixed by switchgrass comes to US$65/metric ton of CO_2. A detailed breakdown of this cost structure for Agro-Sequestration of switchgrass is shown in Table 4.4b. The lower cost for miscanthus is primarily associated with the higher yield (22.5tonne/hectare/year vs 13.5tonne/hectare/year) and carbon density (0.48wt.% vs. 0.44wt.%) of miscanthus compared with switchgrass.

Inspecting Table 4.4a it is seen that for miscanthus ~50% of the Agro-Sequestration costs come from expenses associated with farming. About 44% of these farming expenses come from rental of the farmland (US$494/hectare/year), 21% of these farming expenses are associated with establishment of the miscanthus crop, and 36% are yearly expenses associated with farming the established miscanthus crop. The remaining Agro-Sequestration CO_2 offset cost for miscanthus (~US$28/tonne CO_2) comes from biolandfill sequestration. Of this ~US$28/tonne of CO_2 approximately two thirds of the cost is associated with operating expenses at the landfill and one

Agro CCS Base Case For Switchgrass	Sequestered Switchgrass Cost US$/Tonne	Cost of Sequestered Carbon US$/Tonne of C	CO_2 Capture Cost Equivalent US$/Tonne of CO_2
Landfill OPEX	33	75	20
Landfill CAPEX	15	35	10
Establishment	3	8	2
Farmland	36	83	23
Farming Cost Post Establishment	17	38	10
Total Sequestration Cost	101	238	65

Table S4.4b: Base case Agro-Sequestration (Agro CCS) cost summary for switchgrass. Cost of sequestered carbon is computed from the sequestered switchgrass price using 44wt.% carbon in dry switchgrass. All costs of sequestered CO_2 employ the molecular weight ratio 12/44 and are rounded to nearest dollar.

third is associated with construction and closure of the landfill. Per tonne of biolandfill CAPEX costs are ~50% lower than conventional municipal landfills because of the high fill density (0.855g/cc vs. 0.3-0.4g/cc).

Inspecting Table 4.4b it is seen that for switchgrass ~54% of the Agro-Sequestration costs come from expenses associated with farming. About 65% of these farming expenses come from payments for the farmland (US$494/hectare/year), ~6% of these farming expenses are from expenses for establishment of the switchgrass crop, and ~30% are yearly expenses associated with farming the established switchgrass crop. The remaining Agro-Sequestration CO_2 offset cost for switchgrass (~US$30/tonne of CO_2) comes from sequestration in the biolandfill. Similarly to miscanthus, approximately two thirds of the biolandfill costs are associated with operating expenses at the landfill and one third is associated with construction and closure of the landfill.

The economic models presented account for cost and amount of carbon sequestered in the biolandfill and multiplies this by the appropriate molecular weight ratio (12/44) to obtain the equivalent direct CO_2 capture cost. This accounting ignores indirect emissions associated with fuels, electricity, plastics, and fertilizers used in the process along with abatements such as carbon captured and stored in plant roots and soil. Some indirect emissions that often come to mind are insignificant. For example, emissions associated with manufacturing all the nested polyethylene geomembranes come to 21 kg CO_2 equivalent per meter^2 of biolandfill. However each meter^2 of biolandfill offsets 47,500kg of CO_2 emissions. This means that the indirect CO_2 emissions associated with manufacture of the polyethylene geomembraes are 0.045% of the direct CO_2 offset from biomass sequestration. There are a large number of factors to be considered for indirect emissions. Depending on the source of energy for fuel and electricity and the credit given for carbon sequestered in plant roots and soil, we estimate that the indirect CO_2 emission costs can range from -5% to +10% of the equivalent direct CO_2 capture costs. As such abatement and avoided cost structures would be scaled by this amount. Due to the wide range of uncertainty, we leave analysis of abatement and avoided costs to future life cycle analyses.

4.5 Economic Sensitivity Analysis and Implications for Other Miscanthus and Switchgrass Agro-Sequestration Technology Options

As would be expected there is a linear scaling for the Agro-Sequestration cost structure. For example, doubling the capital cost of the biolandfill will add either US$9 or US$10/tonne of sequestered CO_2 equivalent for miscanthus or switchgrass, respectively. The CAPEX cost of the biolandfill scales as the reciprocal of the density of the fill which sets the hectares of the landfill per year needed to support a hectare of farming. Reducing the density of compressed miscanthus from 0.85g/cc to 0.25g/cc produces a cost increase of US$21 per metric ton of sequestered CO_2 equivalent with an increase in the area of the biolandfill of 340%. Such low-density packing can come from using farm bailing equipment rather than high density quasi-static and dynamic compression. Farm bailing equipment may be able to produce rectangular stackable bales with a density near 0.25g/cc. For such bales biolandfill operational costs are estimated to be 40% lower than in the base case giving a net cost increase of US$17 per metric ton of sequestered CO_2 equivalent for miscanthus. Similarly for switchgrass there would be a net cost increase of US$18 per metric ton of sequestered CO_2 equivalent.

A case highlighting the impact of the US$494/hectare/year farmland cost reduces it to US$185/hectare/year, which is the average cost under the US Conservation Reserve Program. This would reduce the Agro-Sequestration price by US$8/tonne of sequestered CO_2 equivalent for miscanthus and US$14/tonne of sequestered CO_2 equivalent for switchgrass. The greater reduction for switchgrass is due to its lower productivity per hectare. Currently ~10^7 hectares of farmland is enrolled under the Conservation Reserve Program (CRP) and removed entirely from agricultural production. If it were used to grow plants for Agro-Sequestration, it might offset ~6% of US greenhouse emissions in a futuristic scenario where worldwide emissions rise to 50gigatonne CO_2 equivalent/ year.

Changing crop yields primarily affects land costs and post establishment farming costs. To a rough approximation these costs (land and post establishment farming) scale as the reciprocal of the crop yield and at a given crop yield miscanthus and switchgrass have very similar costs. This surprising similarity is due to a variety of offsetting effects. It is seen that increasing crop yields

to the high-end of the ranges suggested at the beginning of Section 4 reduces the Agro-Sequestration cost by ~10-20%. Dropping crop yields to the low-end of the ranges suggested at the beginning of Section 4 without adjusting land costs to that for marginal land increases the Agro-Sequestration cost by ~30-200% with the higher range coming from switchgrass. When land cost is adjusted to US$75/acre that might be representative of marginal land with productivity at the lower end of the spectrum of crop yields, the increase in Agro-Sequestration cost drops to 10% to 25%.

Trading off salt addition for more thermal drying has a small effect on Agro-Sequestration costs. For an equivalent final water activity decreasing $CsCl_2$ salt addition and increasing thermal drying adds less that 3% to the overall costs for Agro-Sequestration. Decreasing water activity in the dried biomass to ~0.4 adds 10% to overall Agro-Sequestration costs. If a water activity of 0.75 is acceptable, then Agro-Sequestration costs could drop by 10% by using NaCl as a drying agent.

Doubling fertilizer usage changes the overall costs for Agro-Sequestration by ~1%.

Land and crop yield by far represent the greatest sensitivities to the agricultural portion of the Agro-Sequestration costs. Many other sensitivities have been computed and for the purpose of a simple discussion, sensitivities between the two crops (switchgrass and miscanthus) will be discussed here in aggregate. Both miscanthus and switchgrass have a multiyear establishment period during which there is no or limited Agro sequesterable crop. As such the reference cases are sensitive to the time value of money and total sequestered costs drop by ~5-10% if the real rate of return is changed from 6% to 3%. Increasing the assumed project lifetime (crop lifespan) by ~25% results in a decrease of ~5% in the captured CO_2 cost. The current model harvests the crops as silage. Changing the harvesting method to the way in which hay is harvested (mowing, windrowing, and bailing) increases the agricultural costs by ~10%. Increasing the biolandfill construction and closure cost by 50% increases the Agro-Sequestration cost by ~20%.

Base cases presented have been developed for near term scenarios but inflation adjusted costs are expected to drop in the future. These cost reductions are expected to come from many sources. A Moore's Law behavior for agriculture will likely reduce crop prices. As an "experience curve'

develops for Agro-Sequestration and the scale of landfill operations grows additional cost reductions would be expected. In some futuristic scenarios the scale of biolandfill operations can be 10 times greater than the base case, providing economies of scale.

Quantifying uncertainty in the Agro-Sequestration cost structure is complex because of the number of model parameters and the way in which these change with location. Base case scenarios presented here have been developed for the near term, but costs are expected to drop. To address this, we used the sensitivity analysis presented to look at a large number of possible cases for the agricultural portion (crop establishment, post establishment farming, and land) as well as the biolandfilling portions. Specific cases were then chosen to bracket the preponderance of cases considered.

To bracket the lower end of agricultural costs we chose a case with crop yields at the upper end of the reported range (35tonne/hectare/year for miscanthus and 20tonne/hectare/year for switchgrass) and low land cost under the conservation reserve program. Bracketing the preponderance of cases run at the higher ranges of agricultural costs we chose cases run with crop yields at the low-end of the reported range (9tonne/hectare/year for miscanthus and 4tonne/hectare/year for switchgrass) and land cost representative of poorer agricultural land. Brackets for the high-end and low-end agricultural costs for miscanthus and switchgrass are graphically displayed in Figure 4.5a. The lower bracket for CO_2 offset cost for Agro-Sequestration production of miscanthus comes to US$17/tonne of CO_2. For switchgrass the lowest Agro-Sequestration agricultural production cost is higher by US$1/tonne of CO_2 (agricultural production offset cost of US$18/tonne of CO_2). The high-end CO_2 offset cost bracket for agricultural production of miscanthus comes to US$41/tonne of CO_2 and the high end bracket for switchgrass comes to US$45/tonne of CO_2.

In a similar manner we have run a large number of cases to bracket potential ranges of costs for the biolandfill. What is thought to be upper and lower bounds for the sum of OPEX and CAPEX costs was determined by examining the preponderance of probable cases, and specific cases were then chosen as examples that bracket this range. These cases considered alternative methods of compression such as briquetting and also considered the possibility of plastic wrapping

or bagging compressed biomass. A case which brackets the higher end of biolandfill costs is one in which the CAPEX and OPEX costs are increased by 50%. This corresponds to a case in which the base case OPEX costs are fixed, and the CAPEX costs are increased by a factor of ~2.5. A case which brackets the lower end is one in which the OPEX and CAPEX costs are reduced by a third. Brackets for these high- and low-end biolandfill costs for miscanthus and switchgrass are graphically displayed in Figure 4.5a. The lower bracket for CO_2 offset cost for an Agro-Sequestration biolandfill comes to US$17/tonne of CO_2 for miscanthus and US$19/tonne of CO_2 for switchgrass. The high-end bracket for CO_2 offset cost for an Agro-Sequestration biolandfill comes to US$41/tonne of CO_2 for miscanthus and US$43/tonne of CO_2 for switchgrass.

Figure S4.5a: Base case bottom-up analysis of Agro-Sequestration costs for miscanthus, switchgrass, and pine along with brackets covering a wide range of likely scenarios. Details of the bottom-up analysis are presented in SI Sections 4 and 5. Tables S4.1a, S4.1b, S4.1c, S4.1d and S4.4a summarize analysis for agricultural CO_2 capture from miscanthus farming. Tables S4.2a, S4.2b, S4.2c, S4.2d and S4.4b summarize analysis for agricultural CO_2 capture from switchgrass farming and Table S5 summarizes analysis for agricultural CO_2 capture associated with Loblolly pine forestry. Biolandfilling costs are summarized in Tables S4.3a, S4.3b, S4.3c, S4.4a, S4.4b and S4.4c. Bottom-up costs are in general agreement with scaling arguments for agricultural and biolandfill costs as presented in SI Section 6.

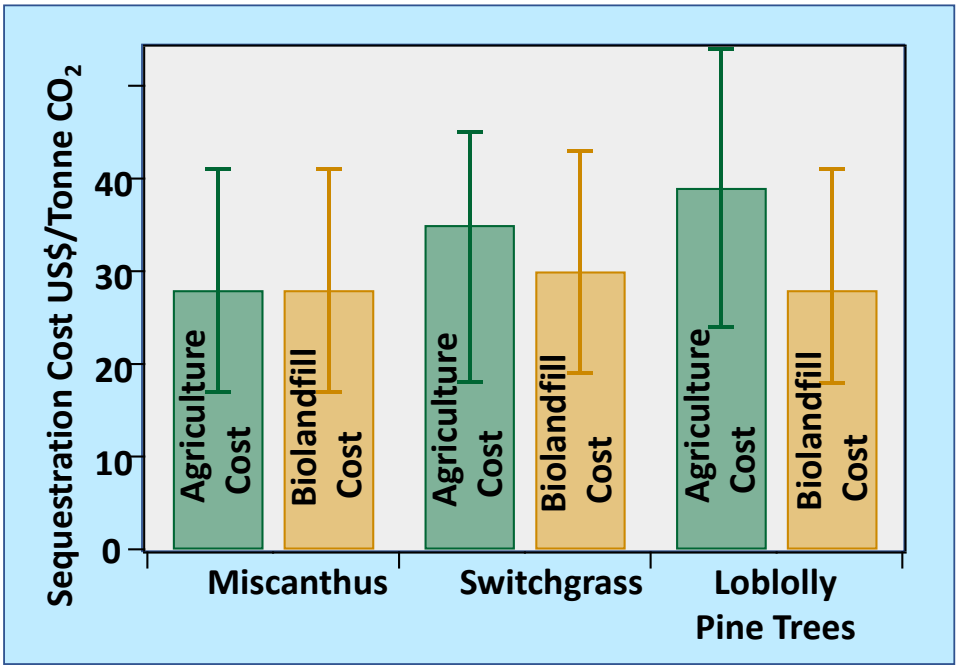

5. Analysis of Agro-Sequestration Costs for Pine Trees

Pine forests have green wood yields in a range from 2-9tonne/hectare/year with the recently improved loblolly pine [72] having a yield of ~9tonne/hectare/year. Cost structure for harvested wood is sensitive to the ways in which a forest is managed, stumpage charges (values placed on standing trees), and green tree water content. Depending on species and location water content in fresh green pine trees can range from ~40wt.% to ~60wt.% compared to the mass density of completely-dry trees. Forestry economics are based on stumpage, harvesting, and transportation charges for fresh green trees and as such include a significant charge for water content. For a base case estimate of pine tree Agro-Sequestration costs we consider loblolly pines and take the green tree water content to be 45wt.% relative to the mass density in completely dry pines. Approximately 2/3 of this water is taken to be located in macropores and larger mesopores that can be emptied by air drying leaving ~15-20wt. % adsorbed water that can come out with heated drying. For a base case model, we take the delivered price at the biolandfill of chopped pine green tree pulpwood to be ~US$40/tonne which includes charges for stumpage, forest harvesting, and transportation. This base case price corresponds to a delivered price of ~US$72/dry tonne and is in a range given in many marketing reports, as well as inflation adjusted analyses of the cost structure of forestry harvesting [124, 125]. Because of the high carbon content in dry pine (~50wt.%) this corresponds to an equivalent CO_2 cost of US$39/tonne of CO_2 which is slightly larger than the base case agricultural cost for switchgrass.

In the base case model chopped pine arriving at the biolandfill is stored for ~ 5 months in a manner that allows it to air dry achieving a moisture level of ~20wt.%. Costs of this air-drying storage are estimated to be similar to the base case model for miscanthus and switchgrass storage. Once air dried, processing for the biolandfill begins with a heated drying step that reduces water content to ~10-12wt.%. It is estimated that the cost of this heated drying is slightly greater than the base case miscanthus model. The almost dry chopped wood is then put into the biolandfill using a combination of quasi-static and dynamic compaction in the same manner as miscanthus or switchgrass, filling to a density of ~ 0.85g/cc.

Putting these values into a discounted cash flow calculation results in an Agro-Sequestration cost for pine of US$62/tonne of CO_2 equivalent and details of the cost structure are summarized in Table S5. Inspecting Table S5 it is seen that ~12% of the pine Agro-Sequestration cost comes from biolandfill CAPEX, ~30% of the pine Agro-Sequestration cost comes from landfill OPEX and the remaining ~58% comes from the cost of green timber at the biolandfill.

Economic sensitivity analyses were run around this base case and, as would be expected, there is a linear scaling for the cost structure for pine tree Agro-Sequestration. Sensitivities considered

Agro CCS Base Case For Loblolly Pine	Sequestered Pine Cost US$ / Dry Tonne	Cost of Sequestered Carbon US$/Tonne of C	CO_2 Capture Cost Equivalent US$/Tonne of CO_2
Landfill OPEX	37	75	20
Landfill CAPEX	15	31	8
Green Wood Arriving At Biolandfill	72	143	39
Total Sequestration Cost	124	249	68

Table S5: Base case Agro-Sequestration (Agro CCS) cost summary for Loblolly pine. Cost of sequestered carbon is computed from the sequestered dry pine price using 50wt.% carbon in dry wood. All costs of sequestered CO_2 employ the molecular weight ratio 12/44 and are rounded to nearest dollar.

for green pine delivered at the biolandfill were ±US$15/tonne. This would increase or decrease the Agro-Sequestration cost by ~US$15/tonne CO_2 equivalent. Increasing the landfill CAPEX and OPEX by 50% would change the Agro-Sequestration cost by US$13/tonne CO_2 equivalent. Decreasing the landfill CAPEX and OPEX by a third would change the Agro-Sequestration cost by US$10/tonne CO_2 equivalent.

We used the economic sensitivity cases which have been discussed to provide bounding estimates for the Agro-Sequestration cost structure for pine. Bounding cost estimates for forestry (agriculture) and biolandfill charges are shown in Figure 4.5a.

6. Scaling Relationships That Provide a First Estimate of Crop and Biolandfill Costs

There are many ways of using scaling relationships to make a rough estimate of crop and landfill costs for Agro-Sequestration. In this section an approach which uses data from prices farmers received for four major row crops in the United States (corn, wheat, soybeans and alfalfa hay) along with costs of municipal landfills is presented to provide a check and perspective on the detailed bottom up estimates which were also based on US cost models.

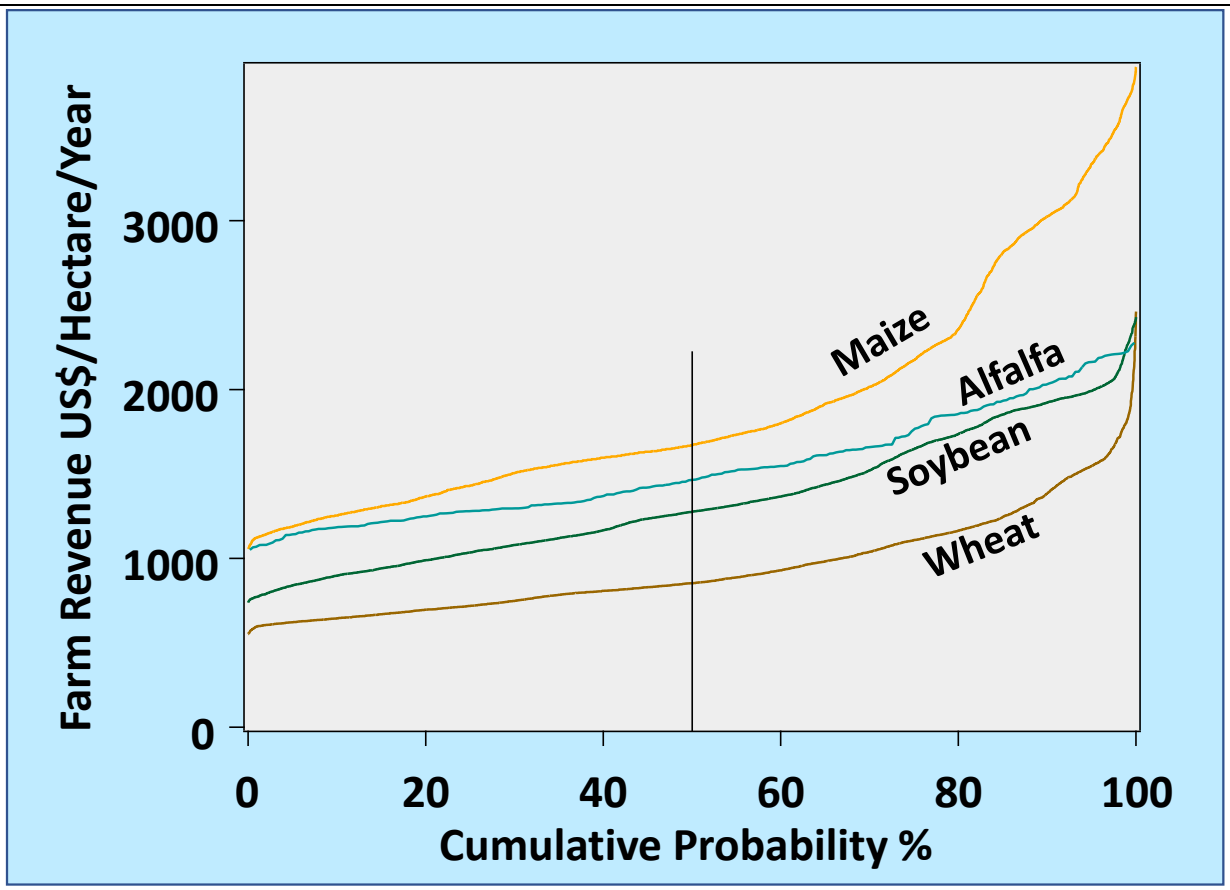

Figure S6.a: The vertical axis shows inflation adjusted yearly farm revenue per hectare for corn, wheat, soybeans, and alfalfa hay derived from historical crop prices and yields, and the horizontal axis is the cumulative probability distribution. Median values are taken as representative of farm incomes that support different types of farming. Median farm revenues are used to form a rough estimate of the agricultural CO_2 capture cost. Scaling of median farm incomes to equivalent agricultural CO_2 capture costs is a purely economic exercise and does not imply that farmland use for food production will be repurposed and used for Agro-Sequestration.

Prices farmers receive for major row crops must cover their costs, revealing the cost structure of agriculture. Nonetheless, price fluctuations due to market conditions, are greater than fluctuations in farming cost. We use the median prices as a surrogate for farming costs, but this almost certainly over-estimates costs since farmers would insist upon being profitable in most years, not half the years, as represented by the median.

Figure S6.a shows the cumulative probability distribution of inflation adjusted yearly revenue farmers received from corn, alfalfa hay, soybeans and wheat over the last 22 years. Yearly farm revenue is expressed as US$/hectare of farmland and is computed from sales prices and average crop yields of 4, 10, 3.1, and 7.8 tonne/hectare/year for wheat, corn, soybeans, and alfalfa hay respectively. Underlying data used to prepare the graph [126, 127, 128, 129] comes from the US Department of Agriculture, the Chicago Board of Trade, and Macrotrends. Crop price data was inflation adjusted to reflect dollar value on Jan 1, 2022 using data from the US Bureau of Labor Statistics. In the cumulative probability distribution shown in Figure S6.a, the median value occurs at 50%. At this point 50% of the time there is a higher farm income and 50% of the time there is a lower farm income.

These median values reflecting inflation adjusted farm revenue per acre that support different types of farming are shown in Figure S6.b (left axis). To provide a simple perspective on the market conditions under which farmers must be able to economically produce crops, brackets are shown in Figure S6.b (left axis) that span the lower quartile to the upper quartile in the distributions of yearly farm income.

A rough estimate of agricultural direct air capture costs can then be calculated from the farm revenue per acre for food crops by assuming that the farm revenue comes from growth of energy crops with 22.5 dry tonne/hectare/year and 50wt.% carbon. This is not meant to imply that farmland used to produce food is to be repurposed for growth of energy crops. Rather it is purely an economic scaling argument that quantifies how much income a farmer must receive from CO_2 credits to have an identical median income. The 22.5 dry tonne/hectare/year is identical to the crop yield in the base case miscanthus model. With this crop yield per hectare, the revenue (US$/hectare/year) on Figure S6.b (left axis) can be converted to revenue/tonne CO_2 on Figure S6.b (right axis). Numerically this conversion (left axis to right axis) amounts to multiplying the left-hand axis by 0.0243Hectare/CO_2-tonne year.

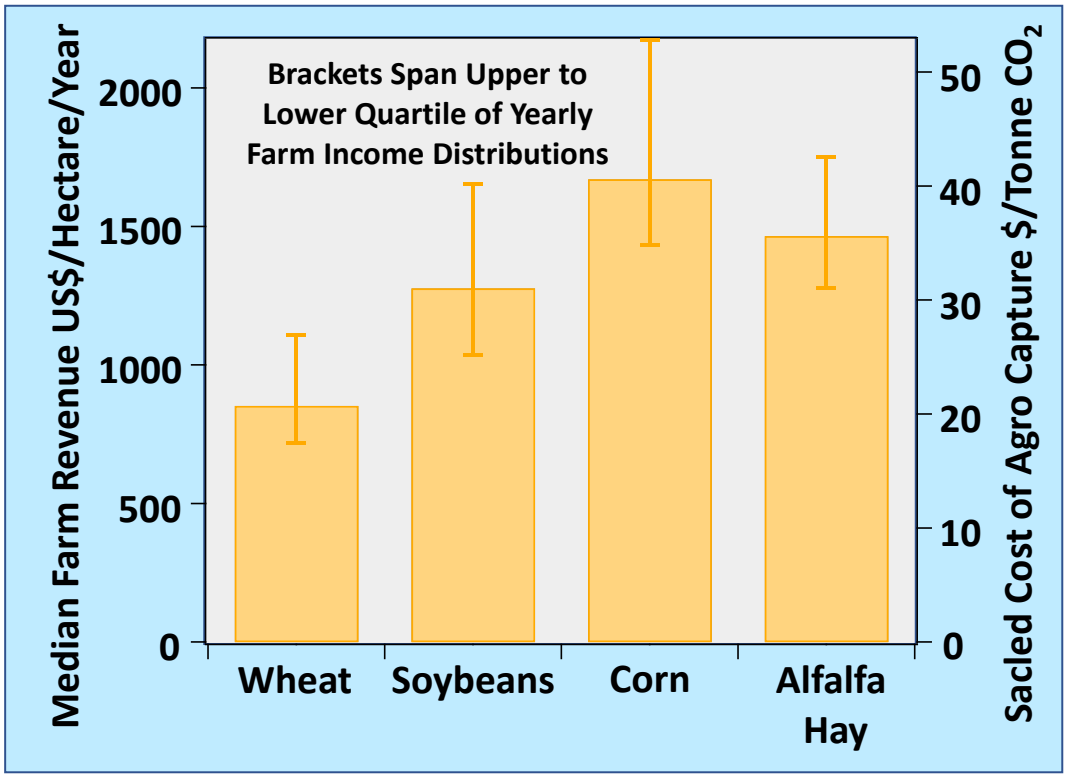

Figure S6.b: Left axis gives median values taken from the cumulative probability distribution (shown in Figure S6.a) of inflation adjusted farm revenue per hectare. These median values are considered to be representative of revenue that supports different types of farming. A perspective on the market conditions under which farmers economically produce crops is shown with brackets that span the lower quartile to the upper quartile in the distributions of yearly farm income. The right axis scales the left axis to an equivalent agricultural CO_2 capture cost by assuming energy crop yield of 22.5 dry tonne/hectare and 50wt.% carbon content. The conversion factor from the right axis is 0.0243Hectares/CO_2-tonne year. The right axis is a result from purely economic scaling and does not mean that farmland used to grow food crops is used for Agro-Sequestration.

Covering the median revenue range from different food crops US$850-1700/hectare/year, the corresponding range for agricultural CO_2 capture is US$20-40/$CO_2$-tonne. Averaging the median estimation of CO_2 capture costs gives US$32/metric ton of CO_2 and as a rough estimate we take the agricultural CO_2 capture price to be US$30/metric ton of CO_2.

Rough estimates of the cost for CO_2 capture based on median farm revenue shown in Figure S6.b (right axis) are broadly similar to the agricultural CO_2 capture costs for the bottom-up

miscanthus, switchgrass, and pine models shown in Figure S4.5a. Even though these costs are arrived at in a very different manner, we take this agreement as a consistency check between the scaling analysis and the bottom-up analysis. As might be expected the range of agricultural scaling for CO_2 capture costs based on median farm income is larger than the range spanning the bottom-up miscanthus, switchgrass, and pine models. Brackets covering the range of CO_2 capture costs for the bottom-up models (Figure S4.5a) overlap almost exactly with the brackets shown in Figure S6.b (right axis) that span the lower quartile to the upper quartile CO_2 capture costs based on farm income. Even though this is a much weaker comparison it supports the view that there is a reasonable degree of consistency between the bottom-up model and the scaling analysis of agricultural CO_2 capture costs.

A rough estimate of biolandfill costs can be arrived at from an analysis of tipping fees at municipal landfills in the US. The average tipping fee in 2021 was approximately US$60/tonne with a variation ranging from +60% to -30% depending on location [130]. The majority of the tipping fee (~66%) is associated with CAPEX for construction and closure. To compare to the CAPEX for Agro-Sequestration, the municipal landfill CAPEX has to be rescaled because of differences in density of the fill. Compacted US landfills are reported to have a density in a range from 0.3 to 0.4g/cc [59] while base case Agro-Sequestration biolandfills for miscanthus and switchgrass have densities of 0.85g/cc. Rescaling the average US municipal landfill cost by the density ratio and the fraction of tipping fees associated with CAPEX we arrive at a rough biolandfill CAPEX estimate in a range from US$13-19/tonne of dry biomass for construction and closure. By comparison the base case bottom-up analysis for miscanthus and switchgrass has a CAPEX cost of US$15.5/tonne of dry biomass. This again shows consistency between the bottom-up model and our rough cost estimates. The CAPEX portion of the biolandfill CO_2 capture cost thus ranges from US$7.50-10/tonne of CO_2 which is arrived at by dividing the cost per tonne of biomass by a molecular CO_2 equivalence factor of 1.83 metric ton of CO_2 per metric ton of biomass.

The OPEX portion of the biolandfill expenses is larger than that for municipal landfills because of additional storage, drying, dry filling, and compaction costs. The added charges are expected to increase the OPEX encountered in municipal landfills by a factor 1.5 to 2.5. Using

this to rescale municipal landfill OPEX we arrive at a biolandfill OPEX cost of US$31/tonne of biomass to US$52/tonne of biomass. The OPEX portion of the estimated CO_2 equivalent capture cost thus ranges from US$17-28/tonne of CO_2 which is again arrived at by dividing the cost per ton of biomass by a CO_2 equivalence factor of 1.83.

As such the overall CO_2 capture and sequestration charge (CAPEX+OPEX) for biolandfilling ranges from US$24-38/tonne CO_2 equivalent which encompasses a large fraction of the bottom-up cases. Within the accuracy of our model we take the biolandfill sequestration charge to be US$30/tonne CO_2, providing a rough estimate of overall CO_2 capture and sequestration costs of US$60/tonne CO_2.

Depending on the energy source for fuel and electricity and the credit given for carbon sequestered in the roots and soil, we estimate that the indirect CO_2 emission costs can range from -5% to +10% of the equivalent direct CO_2 capture costs. As such abatement and avoided cost structures would be scaled by this amount. Similarly, the carbon efficiency for agricultural carbon capture and sequestration can range from 90% to 105% of the carbon sequestered in the biolandfill. Due to the range of uncertainty, we leave analysis of abatement and avoided costs to future life cycle analyses.

7..Water Transport Through Cap and Base Water Permeation Barriers

In early landfill designs compacted clay liners were used to limit water permeation. Water transport through compacted clay and geosynthetic clay liners has been extensively studied [131, 132, 133, 134, 135, 136, 137] with transport described by Darcy's law [138] having a linear response to hydraulic head height (Δh);

$$J = k\ Area\ \frac{\Delta h}{L}$$

where J (m^3/s) is the water flux, k (m/s) is the hydraulic permeability, and L (m) is the thickness of the compacted layer. It has been argued that the dominant underlying transport mechanism is purely diffusive [139], however treatments that have been used are Fickian and have several pitfalls when the feed and permeate are liquids [140].

To an engineering approximation, the Darcy's law treatment provides a way to predict performance targets for transport through clay layers. Studies of excavated cap structures from landfills [134, 135, 136, 137] indicate that degradation of cap barrier properties is primarily responsible for water invasion. In these studies, the hydraulic head height driving water permeation into landfills appears to be less than 1 meter. At the time of instillation geosynthetic clay caps can be engineered to have permeabilities of less than 5×10^{-11}m/s [135]. For reported hydraulic head heights, this permeability would deliver an equivalent water layer with a thickness of less than 1.5mm/year everywhere across the entire surface of a freshly installed meter thick geosynthetic clay cap. This is deemed to be an unacceptable amount of water delivery for Agro-Sequestration and after cap degradation it would be many orders of magnitude higher.

In the laboratory permeability of bentonite [131] is found to be more than 100 times lower giving a permeation rate that delivers an amount of water equivalent to less than a 15μm thick layer of liquid per year everywhere across the surface of a fresh meter thick bentonite cap, however significant deterioration is expected in field settings. Degradation of clay barrier properties has been traced to several factors including exchanging Na ions with Ca ions in the clay structure and cyclic hydration and dehydration of the clay cap from weather and other events which leads to cracking. Because of these instabilities we propose adopting more recent engineered landfill designs that primarily rely on using plastic geomembranes to prevent permeation of water into the landfill [141, 142, 143, 144, 145]. Current designs use 1.5-3mm thick low permeability plastic sheets welded together to form the geomembrane.

A variety of low permeability plastics have been used including high-density polyethylene, low-density polyethylene, linear low-density polyethylene and polypropylene. Significant technology advances have occurred and continue to occur, in the formulation of resins to make these geomembranes, as well as the ability to weld sheets together, and methods that detect imperfections in the welded seams through which water could hydraulically flow. For Agro-Sequestration we propose having at least two layers of plastic geomembranes on all faces of the biolandfill to mitigate permeation defects that might occur in seams where plastic sheets are welded together. To prevent any defect leakage from one membrane to another, we propose having a relatively low permeability layer between the geomembranes. Candidate materials for

the low permeability layer between geomembranes include clays, clay sand mixtures, soil, and geosynthetic clay membranes.

For a base case design we consider geomembranes formed from ~2 mm thick linear low density polyethylene (LLDPE) sheets. If there are no defects in the seam welds, transport of water through the geomembrane is purely diffusive with no hydraulic contribution. As such, the upper bound limit of flux can be determined from membrane permeation rates of saturated water vapor (100% relative humidity) across polyethylene sheets of known thickness to a dry side (0% relative humidity). Because polyethylene sheets are commercially used as vapor and moisture barriers in construction and packaging industries there are a large number of measurements of the Water Vapor Transmission Rate (WVTR) at high relative humidity and it is a specification quoted for many commercial product offerings [57]. Some measurements of the WVTR are done with feeds at 100% relative humidity transporting to a cell with ~0% relative humidity and we chose to use a set of measurements at 38C for an 89μm thick 0.94g/cc polyethylene film [58]. Scaling this data set to the ~2mm thick geomembrane used in our design case, the permeation from liquid water would deliver an amount in one year equivalent to a ~30 micron thick film on the rear surface of the geomembrane (if the water activity on one side was 1 and almost 0 on the other side). Water delivery rates would be a factor of ~2 lower for higher density (~0.96g/cc) polyethylene. The design case has two 0.94g/cc geomembranes and with no mass transfer resistance in the layer between them the water delivery rate is half this amount (a 15μm thick film per year) for the large water activity gradient used in the test conditions. The design case has a spacer layer between them which has significant mass transfer resistance. This mass transfer resistance comes from the geosynthetic clay, geocomposite and soil layers and produces a less steep gradient of water activity. These mass transfer resistances are estimated to decrease the water transmission rate by a factor of ~3. In addition, there will be significantly less driving force for water permeation than in the WVTR tests. On the exterior surface of the water transmission barrier the activity of water is on average expected <1. Within the dry tomb structure, the water activity will be somewhat less than 0.6. With a change of water activity across the water transport barrier from 1 on the exterior surface to 0.6 on the interior surface, the water transport rate will decrease by a factor greater than 3. Incorporating the drop in the water transmission rate from mass transfer resistances in the spacer layers, the overall drop in the water vapor transmission rate is expected to be greater than a factor

9 compared to the 15mμ thick liquid film delivered with no additional mass transfer resistances under the WVTR test conditions. As such the water delivery rate into the biolandfill is expected to be equivalent to less than a ~1.75μm thick water film per year coating the interior surface of the water transport barrier (top or bottom seal). We observe that at this permeation rate, less than 1.75kilogram of water would be delivered across each square meter of top and bottom seal into the dry tomb structure in 1,000 years. In our design case each square meter at the bottom of the ~30meter thick dry tomb supports 25,000kilograms of compressed biomass salt composite. If the biomass salt composite in the dry tomb had 10wt.% water then this amount of biomass salt composite would contain 2,500kilograms of water. As such in our design case the amount of water delivered across the top and bottom seals is expected to be more than 400 times less than the amount of water contained within the dry tomb. (It should also be noted that in the base case design we have also made provision for overlaying a geosynthetic layer on the geomembrane liner which has been reported to improve stability [146].)

8. Scenario for Sequestration of 500Megatonnes/Year of Biomass in the United States and Agro-Sequestration CO_2 Footprint

This section presents a detailed look at one of many possible scenarios showing how Agro-Sequestration could be scaled in the United States to sequester 500megatonnes/year of biomass, offsetting ~925megatonnes of CO_2 emissions per year. The scenario is based on the DOE's 2016 Billion Ton Report [71] and is but one of an infinite set of possible options. Choice of a single scenario at this scale is meant to give a better regional understanding of what could reasonably be achieved with the Agro-Sequestration approach. It provides a focused discussion of available biomass resources and Agro-Sequestration requirements that can be summarized in a brief discussion with manageable sized tables.

Our scenario is based on potential additions of biomass from a variety of different sources (Energy Crops, Forestry Resources, Agricultural Residues and Waste Resources) that could potentially be made available by 2040 at a price of $60/ton or less. The DOE's Billion Ton report [71] provides specific information about these resource additions including their location. From this resource base we picked a scenario (shown in Table S8.1) that relies heavily on energy crops and forests as a biomass source, but incorporates some contribution from agricultural residues and

waste resources. Incorporation of agricultural residues and waste resources acknowledges their surprisingly large potential.

Table S8.1 Distribution of biomass sources for a hypothetical scenario sequestering 500 megatonnes/year of biomass with Agro-Sequestration in the US.

Biomass Source	Potential US Biomass Additions by 2040 DOE Base Case [a]	Hypothetical Scenario Sequestering 500 Megatonnes of Biomass	Percent of Base Case Potential Used In Scenario
	(Megatonnes)		
Energy Crops	374	320	86 %
Forestry Resources	88	80	91 %
Agricultural Residues	160	70	38 %
Waste Resources	129	30	31 %

a. From Table ES1 in DOE 2016 Billion Ton Report.

Table S8.2 Distribution of energy crops chosen from potential biomass additions by 2040 listed in DOE Billion Ton report [71].

Energy Crops	Potential US Biomass Additions by 2040 (2% Yield Increase)[a]	Hypothetical Scenario Sequestering 500 Megatonnes of Biomass	Percent of Potential Biomass Used In Scenario
	(Megatonnes)		
Miscanthus	255	180	71 %
Switchgrass	163	120	74 %
Noncoppice Wood	148	10	7 %
Coppice Wood	45	10	22 %

a From Figure 4.5 (with 2% yield increase) in DOE 2016 Billion Ton Report.

Most of the sequestered energy crop biomass in our scenario comes from miscanthus and switchgrass with a small fraction of other energy crops listed in the Billion Ton Report [71]. The distribution shown in Table S8.2 uses less than 75% of the projected availability of any energy

crop and significantly weights the importance of switchgrass and miscanthus which were discussed in great detail in SI Sections 3 and 4.

Large amounts of agricultural residues are projected to become available which can be sequestered in a dedicated biolandfill or mixed into biolandfills sequestering energy crops, trees, or waste resources. The distribution of agricultural residues chosen for our scenario is listed in Table S8.3 below and consumes ~50% of the two largest agricultural residue sources projected to be available by 2040. A biolandfill could be dedicated to sequestering agricultural residues in places where more than ~0.25megatonne/year is available within a ~75kilometer radius. Otherwise, agricultural residues would be mixed into biolandfills sequestering other types of biomasses.

Table S8.3 Distribution of agricultural residues chosen from potential biomass additions by 2040 listed in DOE Billion Ton report [71].

Agricultural Residues	Potential US Biomass Additions by 2040 (2% Yield Increase) [a]	Hypothetical Scenario Sequestering 500 Megatonnes of Biomass	Percent of Potential Biomass Used
	(Megatonnes)		
Corn Stover	139	60	43 %
Wheat Straw	18	10	55 %
Barley Straw	1	0	0 %

a From Figure 4.5 in DOE 2016 Billion Ton Report.

Large amounts of waste products are also projected to become available. It is possible to dedicate a biolandfill to sequestering waste products without incurring large transportation costs in places where more than ~0.25megatonne/year is available within a ~75kilometer radius. Otherwise, waste products would be mixed into biolandfills sequestering other types of biomasses. For stable sequestration it is preferred to use waste products that have a reasonable lignin content. The scenario shown in Table S8.4 uses 10% to 40% of potential waste product additions having higher lignin contents that are projected to be available by 2040.

Table S8.4 Distribution of waste products chosen from potential biomass additions by 2040 listed in DOE Billion Ton report [71].

Waste Products	Potential US Biomass Additions by 2040 (2% Yield Increase) [a]	Hypothetical Scenario Sequestering 500 Megatonnes of Biomass	Percent of Potential Biomass Used
	(Megatonnes)		
Orchard and Vineyard Prunings	5	4	38 %
Rice Straw	5	4	20 %
Cotton Field Residues	2	1	25 %
Cotton Gin Trash	1.5	1	33 %
Urban Wood Waste (Construction and Demolition)	23	15	13 %
Urban Wood Waste (MSW)	6	4	33 %
Mill Residues	4	1	25 %

a From Figure 4.5 in DOE 2016 Billion Ton Report.

To provide a perspective on physical characteristics of biolandfills needed for the 500megatonne/year biomass sequestration scenario, we consider biolandfills dedicated to the largest resources (miscanthus, switchgrass and forests). Table S8.5 gives a perspective on the total agricultural land required to grow the amounts of miscanthus switchgrass and forestry resources called for in the scenario sequestering 500megatonnes of biomass (see Tables S8.1 and S8.2). It is seen that producing the amounts of miscanthus and switchgrass needed in our scenario requires 2-3% of US crop and pastureland and the amount of forestry resources needed required 3-4% of US forest and woodlands. In aggregate these three resources offset 0.66gigatonnes of CO_2 emissions.

Table S8.5 Land requirements for production of miscanthus, switchgrass, and trees in scenario sequestering 500megatonnes of biomass.

Biolandfill Characteristics	Hypothetical Miscanthus Scenario	Hypothetical Switchgrass Scenario	Hypothetical Forestry Scenario
Biomass (Megatonne/Year)	180	120	80
Land Required Hectare [a]	8×10^6	9×10^6	12×10^6
% Of Total US Forest, Crop or Pastureland	2-3% Of US Crop and Pastureland	2-3% Of US Crop and Pastureland	3-4% Of US Forests and Woodlands
Equivalent CO_2 Offset - Gigatonne	0.32	0.19	0.15

a. *Biomass productivity of: 22.5 tonne/hectare for miscanthus, 13.5 tonne/hectare for switchgrass and 6.5 tonne/hectare for forests.*

Scale of biolandfill operations in the scenarios presented is set by biomass availability within ~60 to 90kilometers of the biolandfill. This distance was chosen to have a reasonable transportation cost from the point of harvest to the biolandfill. Our scenario assumed that for energy crops 30% of the land area in the region around the biolandfill would be used for production. For forestry it was assumed that 90% of the land around the biolandfill could be harvested. This amount of biomass availability sets the size of biolandfills which is summarized in Table S8.6. If smaller percentages of land are used for biomass production, then the biolandfill scale, (mass sequestered per year), would be diminished and more biolandfills would be needed to meet total production targets of 180megatonne/year for miscanthus, 120megatonne/year for switchgrass and 80megatonne/year for forestry. It should be noted that increasing the number of biolandfills does not increase the total land area required for biolandfilling. Table 8.6 also shows that yearly land requirements for biolandfills are only 0.005% to 0.009% of the land area used for biomass production. This extremely small land requirement is due to the compaction of biomass to 0.85g/cc and a biolandfill design with a fill depth of 30.5 meters (see SI sections 2 and 4.3). In addition, when filled most of the biolandfill surface can be used to grow crops.

Table S8.6 Physical characteristics of biolandfills dedicated to miscanthus, switchgrass, and trees.

Biolandfill Characteristics	Hypothetical Miscanthus Scenario	Hypothetical Switchgrass Scenario	Hypothetical Forestry Scenario
Average Transport Distance to Biolandfill - Kilometer	55	60	45
Assumed Fraction of Neighboring Farmland Used to Produce Biomass	30%	30%	90%
Biolandfill Size Megatonne/Year [a]	4	3	2
Biolandfill Size Hectare/Year [b]	16	12	8
Total Number Of Biolandfills Needed In 500Megatonne Scenario	45	40	30
Total Area Are for All Biolandfills - Hectare	690	460	310
% Of Land Used to Produce Biomass Used for Biolandfills	0.0086%	0.0051%	0.0007%

a. Biomass productivity of: 22.5 tonne/hectare for miscanthus, 13.5tonne/hectare for switchgrass and 6.5tonne/hectare for forests.

b. Biomass compacted to a density of 0.85g/cc with biomass fill depth of 30.5 meters.

To obtain an estimate of CO_2 emissions for Agro-Sequestration one has to account for direct and indirect emissions from agricultural production and transportation of crops or wood as well as from construction and operation of biolandfills. In this accounting, direct emissions are on

site emissions while indirect emissions are emissions associated with production of materials and electricity that are used on site.

In accounting for net CO_2 emissions from agricultural production of energy crops and wood, one has to include credits given for increases in carbon content in the soil and carbon stored in plant roots. In many analyses these more than offset direct and indirect emissions from agricultural production. Because of the variability in the credits given and the extensive discussion in the literature, net CO_2 emissions from production of energy crops and wood will not be addressed here. Instead, we will examine direct and indirect emissions from features that are unique to biolandfills: (1) biolandfill construction, (2) biolandfill operations (drying and biomass compaction), and (3) biomass transportation to the biolandfill. To provide a detailed accounting of emissions, we consider biolandfills dedicated to the largest resources (miscanthus, switchgrass and forests).

The largest potential source of greenhouse gas emissions from biolandfill operations is drying to reduce the water activity below 0.6. Biomass stored at the biolandfill has to be dried before it can be placed into the biolandfill. Table S8.7 presents two cases for heated drying in which different amounts of $CaCl_2$ are added for sequestration. When less $CaCl_2$ is added the amount of heated drying is increased. It should be noted that from a water activity perspective, biomass drying with a large $CaCl_2$ addition (~2wt.%) is very conservative; but from a $CaCl_2$ supply standpoint it is very aggressive. Treating 500megatonnes/year of biomass with 2wt.% $CaCl_2$ requires 10tonnes/year which is more than the world supply. Spot treating and treating regions close to the water diffusion barriers require ~$1/50^{th}$ the amount of $CaCl_2$. As such without expanding the $CaCl_2$ industry this would be the most realistic option.

Table S8.8 summarizes indirect emissions for an electric drying process (see Section 4.3) where dried biomass is sequestered with a large amount of $CaCl_2$ (2wt.%) added throughout its volume. Indirect emissions come from electricity generation and from production of $CaCl_2$. Table S8.8 includes a worst case analysis of emissions in which electricity comes from the grid as well as a more favorable case in which it is produced with renewables. It also assumes that the large amount of $CaCl_2$ came from the Solvay process instead of geological sources. Even in the worst

case analysis it is seen that the indirect emissions are less than 2% to 3% of the mass of CO_2 captured in the sequestered biomass and with renewable electric energy this fall to less than 1%.

Table S8.7 Heated drying requirements to obtain water activity <0.6 for two scenarios with different $CaCl_2$ additions. One scenario has a larger (2wt.%) $CaCl_2$ addition and the other has a smaller $CaCl_2$ addition (spot treatment and treatments near water transport barriers).

Biomass Drying Scenario	Miscanthus	Switchgrass	Forestry
Biomass Water Content After Storage at the Biolandfill	<15wt. % Water Content After Storage	<15wt. % Water Content After Storage	20wt. % Water Content After Storage
Scenario Using Heated Drying and 2wt.% $CaCl_2$ Addition	6wt. % Water Removed By Heated Drying	6wt. % Water Removed By Heated Drying	11wt. % Water Removed By Heated Drying
Scenario Using Heated Drying With Small [a] $CaCl_2$ Treatment	8wt. % Water Removed By Heated Drying	8wt. % Water Removed By Heated Drying	13wt. % Water Removed By Heated Drying

a. *Spot treatment with $CaCl_2$ and $CaCl_2$ application near water transport barrier*

Table S8.9 summarizes indirect emissions for an electric drying process (see Section 4.3) in which a small amount of $CaCl_2$ is added in spot treatments as well as in regions near the water transport barriers. These indirect emissions come from electricity generation and from production of $CaCl_2$. Table S8.9 includes a worst case analysis of emissions in which electricity comes from the grid as well as a more favorable case in which it is produced with renewables. Because a small amount of $CaCl_2$ is required (~$1/50^{th}$ the amount needed in Table S8.8) it is assumed that it can come from geologic sources. In this scenario it is seen that the total of all indirect emissions associated with drying biomass are less than 2% to 3% of the mass of CO_2 captured in the sequestered biomass when electricity is purchased from the grid and fall to less than 0.5% when renewables are used to generate electricity.

Table S8.8 Indirect emissions from drying biomass and adding 2wt.% $CaCl_2$ throughout the entire biolandfill. Indirect emissions are expressed as a percent of the ratio of the mass of CO_2 emitted to the mass of CO_2 captured by the sequestered biomass.

Biomass Drying With Large $CaCl_2$ (2wt.%) Addition	Miscanthus Emissions as % of CO_2 offset from sequestered biomass	Switchgrass Emissions as % of CO_2 offset from sequestered biomass	Forestry Emissions as % of CO_2 offset from sequestered biomass
CO_2 Emission for Electric Drying Using Electricity from the Grid [a]	1.3%	1.3%	2.4%
CO_2 Emission for Electric Drying Using Electricity from Renewables	<0.2%	<0.2%	<0.2%
CO_2 Emission from $CaCl_2$ Production [b]	0.5%	0.5%	0.5%

a. Grid average emissions of 0.37kg of CO_2/kwhr of electricity

b. Indirect emission for Solvay process of 0.5kg of CO_2 per kg of $CaCl_2$

Table S8.9 Indirect emissions from drying biomass and adding a small amount of $CaCl_2$. in spot treatments and in regions near the water transport barriers. Indirect emissions are expressed as a percent of the ratio of the mass of CO_2 emitted to the mass of CO_2 captured by the sequestered biomass.

Biomass Drying With Small $CaCl_2$ Addition	Miscanthus Emissions as % of CO_2 offset from sequestered biomass	Switchgrass Emissions as % of CO_2 offset from sequestered biomass	Forestry Emissions as % of CO_2 offset from sequestered biomass
CO_2 Emission for Electric Drying Using Electricity from The Grid [a]	1.7%	1.7%	2.8%
CO_2 Emission for Electric Drying Using Electricity from Renewables	<0.3%	<0.3%	<0.3%
CO_2 Emission from $CaCl_2$ Production [b]	<0.1%	<0.1%	<0.1%

a. Grid average emissions of 0.37kg of CO_2/kwhr of electricity
b. Indirect emission for geologic production of $CaCl_2$. Amount required is $1/50^{th}$ the amount needed for the scenario shown in Table 8.8

Direct and indirect emissions associated with biomass compaction and biolandfill construction is very small and is summarized in Table S8.10. Direct emissions come from fuel burned for excavation equipment and equipment used to compact biomass. Indirect emissions come from emissions associated with production of geomembranes, geocomposites, geosynthetic clays and other materials used in construction of the dry tomb structure within the biolandfill. Inspecting Table S8.10 it is seen that direct and indirect emissions associated with biomass compaction and biolandfill construction come to less than 0.3% of the CO_2 offset from the sequestered biomass

Table S8.10 Direct and indirect CO_2 emissions from biolandfill construction and compaction of biomass.

Biolandfill Construction and Compaction Components [a]	Emission Factor	CO_2 Emissions: kg CO_2 Per Square Meter of Landfill	Emissions as % of CO_2 offset from sequestered biomass
Water Diffusion Barriers (Total 8 mm Polyethylene)	3 kg CO_2 / kg Polyethylene	21	0.045%
Geomembranes and Geocomposites	3 kg CO_2 / kg Membrane	42	0.090 %
Fuel for Excavation Compaction	8.8 kg CO_2 / Gallon of Fuel	52	0.11 %
Clay and Geosynthetic Clay	0.22 kg CO_2 / kg Clay	20	0.04%

a. *Our biolandfill design sequesters 26tonne/meter^2 of biomass offestting 48tonne of CO_2 emissions per square meter of the biolandfill (see SI sections 2 and 4.3).*

The final emission that has to be accounted for is direct emission from fuel burned to transport biomass to the biolandfill. A truck carrying ~25tonnes of biomass traveling an average distance of 55kilometer to the biolandfill is expected to emit ~120kilograms of CO_2 per round trip. This emission is ~0.25% of the CO_2 offset from the biomass transported to the biolandfill.

All the direct and indirect emission from construction and operation of biolandfills as well as transportation of crops and wood sum to ~1% to ~3% of the CO_2 offset from the sequestered biomass. Without accounting for agricultural production this would give a carbon efficiency for Agro-Sequestration ranging from 97% to 99% of the carbon sequestered in the biolandfill. Because estimation of emissions and credits in agricultural production are quite varied, we feel that a conservative estimate of the overall carbon efficiency of Agro-Sequestration can range from

90% to 105% of the carbon sequestered in the biolandfill. Owing to the narrow range of uncertainty, further carbon efficiency precision would require analyzing specific projects.

9. Experience Curves and a Moore's Law For Agriculture

Decarbonization and renewable energy technologies that can address the CO_2 problem are in relatively early stages of deployment with many options only in the demonstration or research stage. Going forward it is expected that the scale at which many of these options are practiced will dramatically increase. As the scale increases, a decrease in cost would be expected through the "learning curve", also known as the "experience curve" [147]. Ideally this would lessen the need for a successful Agro-Sequestration technology.

For Agro-Sequestration an "experience curve" is expected as for every technology. Biolandfill construction and operation will most certainly undergo a learning curve, as biolandfill construction is in the early stages. The "experience curve" is expected to reduce some of the biolandfilling cost projections. Large scale biomass production is also expected to be subject to a "learning curve". This is a form of agriculture and there are two measures for agricultural productivity, (a) tonnes per dollar, (b) tonnes per unit land. Famously, the cost of food has gone down, and the tonnes/dollar has gone up. Now <1% of the population can feed the other 99%. Given the need to produce food for an expanding world population and the need for large land areas for Agro-Sequestration the tonnes of biomass per unit land area and tonnes of food per unit land area is most decisive.

Improvements in biomass productivity per unit land area should be expected because attention to productivity of energy crops has only come about in the last 15years with the drive to create second generation biofuels. Improvements in yields for agricultural food production have historically undergone a learning curve that is often overlooked. Some of the best data is the "land productivity of wheat", bushels/acre [148] for which we have data from farms in England, going back before the year 1800, but already showing an exponential improvement.

Gordon Moore observed an exponential increase in the number of transistors/chip with time. Likewise, there are steady improvements in agricultural productivity, which build on previous improvements. Figure 9.1 illustrates this Moore's Law behavior for wheat farming in the United States and Britain. Agricultural productivity in tonnes per hectare has grown ~10 fold in the 225 years since Malthus made his very pessimistic prediction [149] in 1798. During the last century productivity per unit land area has been doubling every 50 years as shown in Fig. 9.1, which is based on data from references [150,], [151], and [152]. Agriculture has its own Moore's Law.

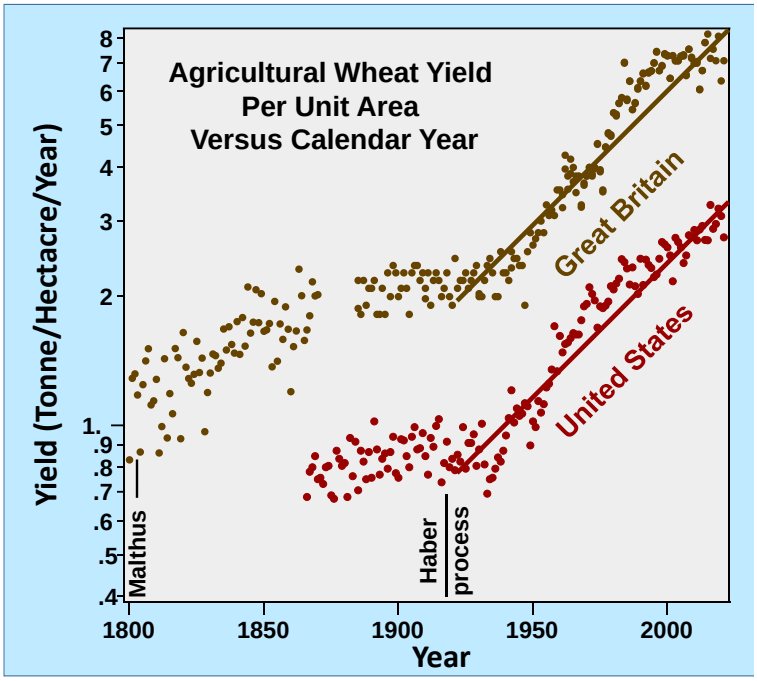

Figure 9.1: There is a Moore's Law for agriculture, but it is much slower than the Moore's Law for transistor density. National governments have paid particular attention to agricultural land productivity. There is good data for wheat in Great Britain, going back hundreds of years. Wheat productivity in tonnes/hectare has been improving, through the "experience curve". Humanity has 10000years "experience" in agriculture. In the past 100years, the tonnes/hectare has doubled every 50 years, but we are conservatively basing our Agro-Sequestration cost estimates on current agricultural methods, and neglecting the inevitable future improvements.

The steady rapid productivity increase during the past 2 centuries is owed to many factors, including the Haber Process used to produce nitrogen fertilizers, advanced breeding and genetic engineering, insecticides to protect food crops, and many other factors. We have good data for wheat, but the improvements extend to all row crops and most other forms of agriculture. Future improvement will likely arise from CRISPR gene editing technology, [153], among other new approaches. There is room for improvement. The best flat-plate solar panels operate at 30% efficiency, while the best carbon fixation agricultural

efficiency is <4%. Thereby, we expect continued agricultural yield increases for at least the next 100years.

In comparison to row crops, very little work has been done toward bioengineering yields of crops suitable for Agro-Sequestration. As such, the land required for Agro-Carbon-Capture & Sequestration for worldwide CO_2 capture is likely to diminish in the future. Nonetheless, the Agro-Sequestration estimates in this paper, leading to an incremental cost of US$0.53/gallon of gasoline for carbon capture, are based on current costs, and current agricultural practices.

References

1. Encyclopedia of Food Microbiology 2nd Edition, C. Batt, M. L. Tortorello, Eds. (Elsevier, Academic Press, 2014). ISBN 978-0-12-384733-1

2. C. Lee et.al., NaCl-saturated brines are thermodynamically moderate, rather than extreme, microbial habitats. *FEMS Microbiology Reviews* **42**, 672–693 (2018).

3. J. Solchaga, J. Busalmen, and D. Nercessian, Unraveling anaerobic metabolisms in a hypersaline sediment. *Front. Microbiol* **13**, 811432 (2022). https://doi.org/10.3389/fmicb.2022.811432

4. N. Merino et. al., Living at the extremes: extremophiles and the limits of life in a planetary context. *Front. Microbiol* **10**, 780 (2019). https://doi.org/10.3389/fmicb.2019.00780

5. A. Stevenson et. al., Is there a common water-activity limit for the three domains of life? *The ISME Journal* **9**, 1333–1351 (2015).

6. J. Buitink, O. Leprince, Intracellular glasses and seed survival in the dry state. *C. R. Biologies* **331,** 788–795 (2008).

7. A.M. Steiner, P. Ruckenbauer, Germination of 110-year-old cereal and weed seeds, the Vienna sample of 1877. Verification of effective ultra-dry storage at ambient temperature. *Seed Sci.Res.* **5,** 195–199 (1995).

8. J. Shen-Miller, M. Mudgett, J. Schopf, S. Clarke, R. Berger, Exceptional seed longevity and robust growth: ancient sacred lotus from China. *Am. J. Bot.* **82**, 1367–1380 (1995).

9. S. Sallon et. al., Germination, genetics, and growth of an ancient date seed. *Science* **320**, 1464 (2008).

10. O. Pérez-Escobar et. al., Genome sequencing of up to 6,000-year-old Citrullus seeds reveals use of a bitter-fleshed species prior to watermelon domestication. *Molecular Biology and Evolution* **39**, Issue 8, August (2022).

11. E. Greco et. al., Proteomic analyses on an ancient Egyptian cheese and biomolecular evidence of brucellosis. *Analytical Chemistry* **90,** 9673-9676 (2018).

12. R. Patalano, J. Hu, Q. Leng, et. al., Ancient Great Wall building materials reveal environmental changes associated with oases in northwestern China. *Sci Rep* **12**, 22517 (2022).

13. O. Pérez-Escobar et. al., Genome sequencing of up to 6,000-year-old Citrullus seeds reveals use of a bitter-fleshed species prior to watermelon domestication. *Molecular Biology and Evolution* **39**, Issue 8, August (2022).

14. A. Arabhosseini, W. Huisman, J. Muller, Modeling of the equilibrium moisture content (EMC) of Miscanthus (Miscanthus giganteus). *Biomass and Bioenergy* **34**, 411-416 (2010).

15. J. Fitzpatrick et. al., Moisture sorption isotherm study of sitka spruce, larch, willow and miscanthus chips and stems. *Biosystems Engineering* **115**, 474-481(2013).

16. K. Okoh, C. Skaar, Moisture sorption isotherms of the wood and inner bark of ten southern U.S. hardwoods. *Wood and Fiber* **12**, 98-111 (1980).

17. C. Karunanithy, K. Muthukumarappan, A. Donepudi, Moisture sorption characteristics of switchgrass and prairie cord grass. *Fuel* **103**, 171–178 (2013).

18. Y. Chen, J. Cheng, K. Creamer, Inhibition of anaerobic digestion process: a review. *Bioresour Technol*. **99**, 4044-64 (2008). https://doi.org/10.1016/j.biortech.2007.01.057.

19. J. Amelse, P. Behrens, Sequestering Biomass for Natural, Carbon Efficient, and Low-Cost Direct Air Capture of Carbon Dioxide. *Int J Earth Environ Sci* **7**, 194 (2022). https://doi.org/10.15344/2456-351X/2022/194

20. Z. Ha, C. Chan, The water activities of $MgCl_2$, $Mg(NO_3)_2$, $MgSO_4$, and their mixtures. *Aerosol Science & Technology* **31**, 154-169 (1999).

21. P. Wang, K. Pitzer, and J. Simonson, Thermodynamic properties of aqueous magnesium chloride solutions from 250 to600 K and to 100 MPa. *Journal of Physical and Chemical Reference Data* **27**, 971-989 (1998).

22. L. Wadsöa, A. Anderberg, I. Åslundb, O. Södermanb, An improved method to validate the relative humidity generation in sorption balances. *European J. of Pharmaceutics and Biopharmaceutics* **72**, 99-104 (2009).

23. P. Barraclough, P. Hall. The adsorption of water vapour by lithium fluoride, sodium fluoride and sodium chloride. *Surface Science* **46**, 282-417 (1974).

24. D. An, T. Teng, J. Sangster, Vapour pressures of $CaC1_2$-NaCl-H_20 and MgC_2-NaCl-H_2O at 25°C. Prediction of the water activity of supersaturated NaCl solutions. *Can. J. Chem.* **56**, 1853-1855 (1978).

25. M. Ally, Predicting phase diagram of the $CaCl_2 \cdot H_2O$ binary system from the BET adsorption isotherm. *Fluid Phase Equilibria* **268**, 45-50 (2008).

26. L. Guo et. al., A comprehensive study of hygroscopic properties of calcium- and magnesium-containing salts: implication for hygroscopicity of mineral dust and sea salt aerosols. *Atmos. Chem. Phys.* **19**, 2115–2133 (2019).

27. L. Fernández, Global calcium chloride market volume. Statista.com (2022). https://www.statista.com/statistics/1245251/calcium-chloride-market-volume-worldwide/

28. J. Warren, Calcium Chloride (CaCl2) Article 2 of 2: CaCl2 minerals across time and space. saltworkconsultant.com (May 31,2017). https://www.saltworkconsultants.com/downloads/27.%20CaCl2%20brines%202%20of%202.pdf

29. J. Speight, The Solvay process. Chemical and process design handbook (The McGraw Hill Companies, New York, 2002).

30. https://secure.drierite.com/

31. M. Shahbandeh, Global salt production. Statista.com (2022). https://www.statista.com/statistics/237162/worldwide-salt-production/

32. A. Hietala, P. Dörsch, H. Kvaalen, H. Solheim, Carbon dioxide and methane formation in Norway Spruce stems infected by White-Rot Fungi. *Forests* 2015, **6**, 3304-3325 (2015).

33. S. Seibold, et al,. The contribution of insects to global forest deadwood decomposition. *Nature*, **597**, 77–81 (2021). https://doi.org/10.1038/s41586-021-03740-8

34. W. Li, et.al., Methane production through anaerobic digestion: Participation and digestion characteristics of cellulose, hemicellulose and lignin. *Applied Energy* **226**, 1219-1228 (2018).

35. A. Anukam, A. Mohammadi, M. Naqvi, K. Granstrom, A Review of the Chemistry of Anaerobic Digestion: Methods of Accelerating and Optimizing Process Efficiency. *Processes* **7**, 1-19 (2019).

36. F. Beulig, H. Røy, C. Glombitza, B. Jørgensen, Control on rate and pathway of anaerobic organic carbon degradation in the seabed. *PNAS* **115**, 367-372 (2018).

37. M. Milke, Y. Fang, S. John, Anaerobic biodegradability of wood: a preliminary review. Christchurch, New Zealand: 2010 Water New Zealand Annual Conference, 22-24 Sep 2010.

38. IPCC 2019, 2019 Refinement to the 2006 IPCC Guidelines for National Greenhouse Gas Inventories, C. Buendia et. al. eds (IPCC, Switzerland, 2019).

39. N. Zeng, H. Hausmann, Wood Vault: remove atmospheric CO_2 with trees, store wood for carbon sequestration for now and as biomass, bioenergy and carbon reserve for the future. *Carbon Balance Management* **17**, 2 (2022). https://doi.org/10.1186/s13021-022-00202-0

40. G. Mustoe, Non-Mineralized Fossil Wood. *Geosciences* **8**, 223 (2018). https://doi.org/10.3390/geosciences8060223

41. M. Broda, C. Hill, Conservation of Waterlogged Wood—Past, Present and Future Perspectives. *Forests* **12**, 1193 (2021). https://doi.org/10.3390/f12091193

42. A. Ghavidel, T. Hofmann, M. Bak, I. Sandu, V. Vasilache, Comparative archaeometric characterization of recent and historical oak (Quercus spp.) wood. *Wood Science and Technology* **54**,1121–1137 (2020). https://doi.org/10.1007/s00226-020-01202-4

43. M. Monachon et. al., Characterization of model samples simulating degradation processes induced by iron and sulfur species on waterlogged wood. *Microchemical Journal* **155**, 104756 (2020).

44. D. Woolf, J. Amonette, A. Street-Perrott, J. Lehmann, S. Joseph, Sustainable biochar to mitigate global climate change. *Nature Communications* **1**, 56 (2010). doi:10.1038/ncomms1053. ISSN 2041-1723. PMC 2964457

45. J. Tumuluru, Comparison of chemical composition and energy property of torrefied switchgrass and com stover. *Front. Energy Res.* **3**, 46-55 (2015).

46. Lehmann, J., Gaunt, J. & Rondon, M. Bio-char sequestration in terrestrial ecosystems - a review. *Mitigation and Adaptation Strategies for Global Change* **11**, 403-427 (2006).

47. P. Fairley, The biofuel correction course. *Nature* **611**, S15-S17 (2022).

48. A. Maliha, B. Abu-Hijleh, A review on the current status and post-pandemic prospects of third-generation biofuels. *Energy Syst* (2022). https://doi.org/10.1007/s12667-022-00514-7

49. M. Fajardy, A. Köberle, N. Mac Dowell, A. Fantuzzi, BECCS deployment: a reality check. Imperial College Lodon: Grantham Institute Briefing paper No 28 (2019). Available at https://www.imperial.ac.uk/media/imperial-college/grantham-institute/public/publications/briefing-papers/BECCS-deployment---a-reality-check.pdf

50. IPCC, 2019: Summary for Policymakers. In: Climate Change and Land: an IPCC special report on climate change, desertification, land degradation, sustainable land management, food security, and greenhouse gas fluxes in terrestrial ecosystems [P.R. Shukla, J. Skea, E. Calvo Buendia, V. Masson-Delmotte, H.- O. Pörtner, D. C. Roberts, P. Zhai, R. Slade, S. Connors, R. van Diemen, M. Ferrat, E. Haughey, S. Luz, S. Neogi, M. Pathak, J. Petzold, J. Portugal Pereira, P. Vyas, E. Huntley, K. Kissick, M. Belkacemi, J. Malley, (eds.)]. In press.

51. J. Crawford, P. Smith, Landfill Technology (Butterworths, London, 1985).

52. Global Climate Initiative International Best Practices Guide for Landfill Gas Energy Projects (U.S. EPA, Washington, 2012).

53. O. O'Leary, P. Walsh, Landfill cover and liner systems for water quality protection. *Waste Age*. **33**, 124–129 (2022).

54. Landfill liners, Wikipedia (2022) available at wikipedia.org/wiki/Landfill_liner.

55. GRI - GM13 Standard Specification, “Test Methods, Test Properties and Testing Frequency for High Density Polyethylene (HDPE) Smooth and Textured Geomembranes”, Geosynthetic Research Institute (GRI) (2021). Available at www.geosynthetic-institute.org

56. GRI - GM17 Standard Specification, “Test Methods, Test Properties and Testing Frequency for Linear Low-Density Polyethylene (LLDPE) Smooth and Textured Geomembranes”, Geosynthetic Research Institute (GRI) (2021). Available at www.geosynthetic-institute.org

57. K. Yam, "Encyclopedia of Packaging Technology", John Wiley & Sons, (2009). ISBN 978-0-470-08704-6

58. J. Krohn, R. Tate, D. Jordy, Factors affecting the permeability of PE blown films. Plastics – Saving Planet Earth, Proceedings of the SPE 55th Annual Technical Conference & Exhibits, ANTEC ’97, 1654-1658 (1997).

59. D. Duffy, Landfill Waste Compaction Strategies - Tools and Techniques, *MSW Management* (2016) January/February.

60. A. Hadas Soil compaction under quasi-static and impact stress loading. *Soil & Tillage Research* **9**, 181-186 (1987).

61. A. Parsons, Compaction of soils and granular materials. a review of research performed at the transport research laboratory (Her Majesty Stationary Office, London England, 1992) pp. 1-323.

62. R. McDonald, Modelling the mechanical behaviour of municipal solid waste for an engineered landfill using viscoelasticity. (Masters Thesis Ottawa-Carleton Institute for Civil Engineering, 2018).

63. P. Nicholson, “Deep Densification - Dynamic Compaction” in Soil Improvement and Ground Modification Methods, (Elsiver, 2015) pp. 115-147.

64. M. Lay, The history of compaction / histoire du compactage. Part 2. The sheepsfoot roller. (World Road Association, France, 1996).

65. H. Marreiro et. al., Empirical studies on biomass briquette production: a literature review. *Energies* **14**, 8320-8360 (2021).

66. P. Krizan, Biomass Compaction: the effects of pressing chamber design parameters on extrusion quality. (Springer, 2022). ISBN: 978-3-030-89956-1

67. A. Facello et. al., Wood chips compaction: first energetic analysis. *Applied Mathematical Sciences* **8**, 6547 – 6554 (2014).

68. https://www.usgs.gov/media/images/map-worldwide-croplands

69. "Global Forest Resources Assessment 2020 – Main Report" (Food And Agriculture Organization Of The United Nations, Rome Italy) pp. 1-184.

70. Land use in agriculture by the numbers, Food And Agriculture Organization Of The United Nations (2020). https://www.fao.org/sustainability/news/detail/en/c/1274219/

71. U.S. Department of Energy. 2016. 2016 Billion-Ton Report: Advancing Domestic Resources for a Thriving Bioeconomy, Volume 1: Economic Availability of Feedstocks. M. H. Langholtz, B. J. Stokes, and L. M. Eaton (Leads), ORNL/TM-2016/160. Oak Ridge National Laboratory, Oak Ridge, TN. 448p. https://doi.org/10.2172/1271651. Available at http://energy.gov/eere/bioenergy/2016-billion-ton-report.

72. N. Brosse, A. Dufour, X. Meng, Q. Sun, A. Ragauskas, Miscanthus: a fast- growing crop for biofuels and chemicals production. *Biofuels, Bioproducts and Biorefining* **6,** 580-598 (2012).

73. I. Lewandowski, J. Scurlock, E. Lindvall, M. Christou, The development and current status of perennial rhizomatous grasses as energy crops in the US and Europe. *Biomass and Bioenergy* **25**, 335-361 (2003).

74. E. Alexopoulou et.al., Biomass yields for upland and lowland switchgrass varieties grown in the Mediterranean region. *Biomass and Bioenergy* **32**, 926-933 (2008).

75. D. Paudel et. al., Surveying the genome and constructing a high-density genetic map of napiergrass (Cenchrus purpureus Schumach). *Scientific Reports* **8**, 1-11 (2018).

76. H. Nielsen, "Sorrel and reed canary grass in Southern Norway" in Aspects *of Applied Biology **90**, Biomass and Energy crops III*, E.Booth et.al., Eds. (Association of Applied Biologists, Wellesboume, 2008) pp. 75- 79.

77. S. Lowthe-Thomas et. al., Reed Canary-grass - A versatile energy crop for Wales? in *Aspects of Applied Biology **90**, Biomass and Energy crops III*, ed. E. Booth et. al., (Association of Applied Biologists, Wellesboume, 2008) p. 81-86.

78. R. Sheldrick, Tropical pasture and fodder plants (grasses and legumes). *Experimental Agriculture* **14**, 289-298 (1978).

79. R. Tanner, S. Hussain, L. Hamilton, F. Wolf, Kudzu (Pueraria Lobata): Potential agricultural and industrial resource. *Economic Botany* **33**, 400-412 (1979).

80. C. Sheaffer et. al., Alfalfa Management Guide (American Society of Agronomy, Crop Science Society of America, Soil Science Society of America, Madison, 2011).

81. S. Kelchner, Higher level phylogenetic relationships within the bamboos (Poaceae: Bambusoideae) based on five plastid markers. *Molecular Phylogenetics and Evolution* **67**, 404-413 (2013).

82. B. Mola-Yudego, J. Gonzalez-Olabarria, Mapping the expansion and distribution of willow plantations for bioenergy in Sweden: lessons to be learned about the spread of energy crops. *Biomass and Bioenergy* **34**, 442-448 (2010).

83. M. Aylott et. al., Yield and spatial supply of bioenergy poplar and willow short-rotation coppice in the UK. *New Phytologist* **178**, 358-370 (2008).

84. D. Rookwood, D. Carter, M. Langholtz, J. Strieker, Eucalyptus and Populus short rotation woody crops for phosphate mined lands in Florida USA. *Biomass and Bioenergy* **30,** 728-734 (2006).

85. D. Rockwood, A. Rudie, S. Ralph, J. Zhu, J. Winandy, Energy product options for Eucalyptus species grown as short rotation woody crops. *International Journal of Molecular Sciences* **9**, 1361-1378 (2008).

86. V. Girijashankar, Genetic transformation of eucalyptus. *Physiol. Mol. Biol. Plants* **17**, 9-23 (2011).

87. T. Albaugh, R. Rubilar, C. Maier, E.Acuna, R. Cook, Biomass and nutrient mass of Acacia dealbata and Eucalyptus globulus bioenergy plantations. *Biomass and Bioenergy* **97** 162-171 (2017).

88. J. Adams, T. Matney, S. Land, K. Belli, H. Duzan, Incorporating genetic parameters into a loblolly pine growth-and-yield model. *Canadian Journal of Forest Research* **36**, 1959-1967 (2006).

89. A. Rassweiler, D. Reed, S. Harrer, J. Nelson, Improved estimates of net primary production, growth, and standing crop of Macrocystis pyriferain Southern California. *Ecology*, **99**, 2132 (2018).

90. S. Davis, F. Dohleman, S. Long, The global potential for Agave as a biofuel feedstock. *GCB Bioenergy* **3**, 68-78 (2011).

91. S. Matsuoka, L. Rubio, Energy Cane: a sound alternative of a bioenergy crop for tropics and subtropics, in *Sugarcane Biofuels* M. Khan, I. Khan, Eds. (Springer, 2019).

92. B. Caslin, J. Finnan, L, Easso, "Miscanthus Best Practice Guidelines," (Agricultural Food & Development Authority) ISBN 1-84170-574-8 (2011).

93. N. Brosse, A. Dufour, X. Meng, Q. Sun, A. Ragauskas, Miscanthus: A Fast- Growing Crop for Biofuels and Chemicals Production. *Society of Chemical Industry and John Wiley & Sons, Ltd. Biofuels, Bioprod. Bioref.* https://doi.org/10.1002/bbb.1353 (2012).

94. M. Hoque, M. Artz, C. Hart, Estimated cost of establishment and production of miscanthus in Iowa. *Iowa State University Extension and Outreach: Ag Decision Maker* (2014). Available at https://www.extension.iastate.edu/agdm/crops/html/a1-28.html

95. I. Lewandowski, J. Scurlock, E. Lindvall, M. Christou, The development and current status of perennial rhizomatous grasses as energy crops in the US and Europe. *Biomass and Bioenergy* **25**, 335-361(2003).

96. D. Turley, Technology and policy requirements in the drive towards improving bioenergy efficiency. *Aspects of Applied Biology* **90**, Biomass and Energy crops III (2008).

97. B. Diedterich et. al., State and development of bioenergy in the Republic Of Ireland. *Aspects of Applied Biology* **90**, Biomass and Energy Crops III, 27-34 (2008).

98. E. Smeets, I. Lewandowski, A. Faaij, The economical and environmental performance of miscanthus and switchgrass production and supply chains in a European setting. *Renewable and Sustainable Energy Reviews* (2008). https://doi.org/10.1016/j.rser.2008.09.006

99. L. Gibson, S. Barnhart, Switchgrass. *Iowa State University Extension and Outreach* https://store.extension.iastate.edu/product/12610 (2007).

100. K. Jacobs, R. Mitchell, C. Hart, To Grow or not to Grow: A tool for comparing returns to switchgrass for bioenergy with annual crops and CRP. *Iowa State University Extension and Outreach – Ag Decision Maker* (2016). Available at https://www.extension.iastate.edu/agdm/crops/html/a1-27.html

101. H. Elbersen, D. Christian, N. Bassem, W. Bacher, G. Sauerbeck, E. Alexopoulou, I. Piscioneri, P. Visser, D. Van der Berg, Switchgrass Variety Choice in Europe. *Aspects of Applied Biology* **65**, 21-28 (2001).

102. E. Alexopoulou et. al., Biomass yields for upland and lowland switchgrass varieties grown in the Mediterranean region. *Biomass and Bioenergy* **32**, 926-933 (2008).

103. M. Khanna, B. Dhungana, J. Clifton-Brown, Costs of producing miscanthus and switchgrass for bioenergy in Illinois. *Biomass and Bioenergy* **32**, 482-493 (2008). https://doi.org/10.1016/j.biombioe.2007.11.003

104. S. Wang, S. Wang, A. Hastings, M. Pogson, P. Smith, Economic and greenhouse gas costs of miscanthus supply chains in the United Kingdom. *GCB Bioenergy* **4**, 358–363 (2012).

105. M. Jacobson, Z. Helsel, New Bio switchgrass budget for biomass production. *Penn State University Extension: Ag Communications and Marketing* (2014).

106. J. Qualls, Switchgrass production decision tool: background and documentation for an Excel spreadsheet-based decision tool for potential switchgrass producers. *Department of Agricultural and Resource Economics, The University of Tennessee* (2016).

107. L. James, S. Swinton, D. Penninton, A comparison of profitability of cellulosic feedstock crops: switchgrass, mixed-species grass, restored prairie, miscanthus and poplar with corn. *Michigan State University Extension Bulletin* E-3084 (2009).

108. Municipal Solid Waste Landfills. Available at www.epa.gov/landfills/municipal-solid-waste-landfills.

109. R. Cossu, F. Garbo, "Landfill Covers: Principles and Design", *Solid Waste Landfilling Concepts, Processes, Technologies* (Elsevier) ed. R. Cossu, R. Stegmann, 649-676 (2018).

110. K. Hughes, A. Christy, J. Heimlich, Landfill types and liner systems. *Ohio State Extension Fact Sheet- CDFS-138-05* (2008).

111. X. Qian, R. Koerner, D. Gray, "Geotechnical Aspects of Landfill Design and Construction", (Prentice-Hall, Pearson Education 2002).

112. K. Venkatraman, N. Ashwath, Can phytocapping technique reduce methane emission from municipal landfills? *International Journal of Environmental Technology and Management* **10,** 4-15 (2009).

113. K. Leutwyler, Landfill liners of asphalt. *Scientific American*, October 16: Sustainability (2000).

114. L. Demianiuk, A. Demianiuk, Influence of temperature on the quality of briquettes in the giant miscanthus densification process. *Engineering Transactions* **64**, 171–180 (2016).

115. Z. Miao, J. Phillips, T. Grift, S. Mathanker, Energy and pressure requirement for compression of miscanthus giganteus to an extreme density. *Biosystems Engineering* **114**, 21-25 (2013).

116. S. Francik, A. Knapczyk, A. Knapczyk, R. Francik, Decision support system for the production of miscanthus and willow briquettes. *Energies* **13**, 1364 – 1388 (2020).

117. RUF Briquetting Systems Spec. Sheet for Wood and Other Organic Materials: Model RUF 1500. RUF Inc. (2020). Available at www.ruf-briquetter.com

118. D. Duffy, Landfill Economics Part 1: Siting. *MSW Management* **15** (3), 118 (2005).

119. D. Duffy, Landfill Economics Part 2: Getting Down to Business. *MSW Management*, **15** (4), (2005).

120. D. Duffy, Landfill Economics Part 3: Closing Up Shop. *MSW Management*, **15** (5), (2005).

121. G. Wang et. al., Research on an electric energy-saving grain drying system with internal circulation of the drying medium, *Journal of Food Energy Process Engineering* (2020). https://doi.org/10.1111/jfpe.13476

122 D. Maier, F. Bakker-Arkema, Grain drying systems. 2002 Facility Design Conference of the Grain Elevator and Processing Society. (July28-31, 2002, St. Charles, Illinois).

123 W. Edwards, Comparison of Drying Systems. Ag Decision Maker A3-23 Iowa State Extension and Outreach Service (2023). available at https://www.extension.iastate.edu/agdm/crops/html/a2-31.html

124. V. Francescato, E. Antonini, L. Bergomi, "Wood Fuels Handbook: Production, Quality Requirements, Trading." *Italian Agroforestry Trade Association* (2008).

125. F. Pan, H. Han, L. Johnson, J. William, W. Elliot, Production and cost of harvesting, processing, and transporting small-diameter (≤ 5 inches) trees for energy. *Forest Products Journal* **58** (5), 47-53 (2008).

126. US Department of Agriculture, Agricultural Prices, ISSN 1937-4216.

127 US Department of Agriculture, Crop Production, ISSN 1936-3787.

128 Chicago Board of Trade (CBOT).

129. www.macrotrends.net

130. Analysis of MSW Tipping Feed 2020, Environmental Research and Education Foundation, (2020). Available at erefdn.org/product/analysis-msw-landfill-tipping-fees-2

131. N. Sebastian, A. Sindhu, Prediction of Permeability of Compacted Clay Liners. *International Journal of Research in Engineering, IT and Social Sciences* **6**, 42-47 (2016).

132. N. Brazzale, L. Hanckel, L. McBride, P. Nugent, A. Deng, The effects of Polycom on the permeability of compacted clay landfill liners. Technical report, BETTA ROADS, Australia (2014).

133. C. Shackelford, F. Javed, Large-scale laboratory permeability testing of a compacted clay soil. *Geotechnical Testing Journal* **14**, 171-179 (1991).

134. C. Benson, J. Chen, B. Tuncer, W. Likos, Hydraulic conductivity of compacted soil liners permeated with coal combustion product leachates. *J. Geotech. Geoenviron. Eng.* **144**, 04018011 (2018).

135. J. Scalia, C. Benson, Hydraulic conductivity of geosynthetic clay liners exhumed from landfill final covers with composite barriers. *Journal of Geotechnical and Geoenvironmental Engineering* **137,** 1-13 (2011).

136. L. Goladman et. al., Design, construction, and evaluation of clay liners for waste management facilities. Final Report EPA Contract No. 68-01-7310, EPA/530-SW-86-007 (1986).

137. W. Albright et. al., Field performance of a compacted clay landfill final cover at a humid site. *Journal of Geotechnical and Geoenvironmental Engineering* **132**, 1393–1403 (2006).

138. M. Al-Doury, A discussion about hydraulic permeability and permeability. *Petroleum Science and Technology* **28**, 1740-1749 (2010).

139. F. Sánchez, "Water diffusion through compacted clays analyzed by neutron scattering and tracer experiments. Universität Bern (2007).

140. Y. Ma, F. Zhang, H. Deckman, W. Koros, and R. Lively, Flux equations for osmotically moderated sorption−diffusion transport in rigid microporous membranes. *Ind. Eng. Chem. Res.* **59** 5412−5423 (2020).

141. C. Brzozowski, Landfill liners and covers. *MSW Management*, Oct. 1st (2015).

142. B. Sunil, Review on performance of geosynthetic liners in municipal solid waste landfills. *Japanese Geotechnical Society Special Publication*: 15th Asian Regional Conference on Soil Mechanics and Geotechnical Engineering, 2368-2372 (2015).

143. R. Koerner, Traditional vs. exposed geomembrane landfill covers. *Geosynthetics* October 1st, 2012 / Environmental, Feature, Geomembranes (2012).

144. A. Whittle, H. Ling, "Geosynthetics in Construction." in Encyclopedia of Materials: Science and Technology (2002).

145. M. Adams, Landfill Liners. *Waste and Recycling Magazine*: Feature article June 1 (2000).

146. M. Chung, M. Seo, K. Kim, J. Park, Protective effect of overlying geosynthetic on geomembrane liner observed from landfill field tests and inclined board laboratory experiments. *Waste Manag Res*. **24**, 250-9 (2006).

147. R. M. Swanson, A vision for crystalline silicon photovoltaics. *Prog. Photovolt: Res. Appl.* **14**, 443–453 (2006). https://doi.org/10.1002/pip.709 (see Fig. 1)

148. A bushel of wheat is 27.2kg for the kernels alone, to which could be added the mass of stems.

149. T. R. Malthus, "An Essay on the Principle of Population, (1798)" (Penguin Books, 2014).

150. A.Howsman, "United Kingdom Cereal Yields, 1885 Onwards" Department for Environmental Food and Rural Affairs, available at

https://www.gov.uk/government/statistical-data-sets/structure-of-the-agricultural-industry-in-england-and-the-uk-at-june. Deposited 2021.

151. Our World In Data, “Historical Cereal yields in the United Kingdom” available at https://ourworldindata.org/grapher/cereal-yields-uk. Deposited 2021.

152. A.Sowell, USDA Economic Research Service Data form “Wheat Data Yearbook” (2021) https://www.ers.usda.gov/data-products/wheat-data/. Deposited 2022.

153. M. Jinek, K. Chylinski, I. Fonfara, M. Hauer, J. Doudna, E. Charpentier, A programmable dual-RNA–guided DNA endonuclease in adaptive bacterial immunity. *Science* **337**, 816-821 (2012).